Chemoenzymatic Modification of Polyolefins: Surface Oxidation and Identification of Degradation Products

Clara Melin

Supervisors:

Sang Hyun Pyo

Mohamed Ismail

Åsa Olsson

Examiner:

Rajni Hatti-Kaul

Master thesis project

Faculty of Engineering, LTH University

Degree project in Biotechnology – KBTM05

Date: February – June 2026

Abstract

Global plastic production exceeds 400 million tons annually, with polyolefins accounting for nearly half. Their highly stable hydrocarbon backbone makes them highly resistant to degradation, leading to environmental accumulation and significant contributions to plastic pollution. Conventional recycling methods are insufficient to address these challenges, highlighting the need for more sustainable alternatives. This study investigates chemoenzymatic modification of polyolefin films, including LDPE, LDPEa (LDPE with antioxidants), LLDPE and HDPE. Chemical pretreatments, $KMnO_4$/HCl, Fenton oxidation and UVC-Fenton were combined with enzymatic treatment using bacterial (*Bacillus Subtils*, L.CotA) and fungal (*Myceliophthora thermophila*, L.MT), laccases in a TEMPO-mediated system. The resulting modifications of the polymer backbone, surface morphology, elemental composition and thermal properties were evaluated using FTIR, SEM, EDX, DSC, HPLC and GC-MS. Following chemoenzymatic treatment, FTIR revealed oxidation of the polymer backbone. The highest calculated carbonyl index values were 2.50 for $KMnO_4$/HCl combined with L.CotA and 2.01 for Fenton oxidation combined with L.MT. Additionally, UVC treatment enhanced Fenton oxidation and enzymatic treatment with both L.CotA and L.MT. SEM analysis revealed visible surface modification in the form of cracks and particle clusters, EDX confirmed an increase in oxygen content and DSC measurements indicated slight decreases in melting temperature and crystallinity. GC-MS analysis of the reaction mixtures identified oxidised degradation products ranging from C2-C20. L.CotA primarily generated longer oxidised oligomers, suggesting more surface limited modification, whereas L.MT produced a broader range of compounds, including short chain hydroxy acids and polyoxidised intermediates, indicating more extensive modification. These degradation products demonstrated great potential for upcycling into biodegradable polymer or other industrial applications. Overall, LDPE and LDPEa films proved most susceptible to the modification.

Popular Science Summary

Every year, global plastic production exceeds hundreds of millions of tonnes, reflecting the strong dependency on plastic materials today. This is a direct result of their superior properties, including high durability, low cost and light weight. However, the same properties that make plastics invaluable in countless applications also make them highly resistant to degradation. Among the most challenging plastics to degrade are polyolefins, which account for around half of global production. Their resistance to degradation stems from their simple chemical structure, consisting entirely of strong saturated C-C and C-H bonds. The most common polyolefins are polyethylene (PE) and polypropylene (PP). These materials are widely used in everyday life and are found in countless products, including plastic bags, food packaging and containers. This widespread use of single-use plastics generates large amounts of plastic waste. Today, only a small fraction of this waste is collected for recycling and most of it is mechanically recycled into products with lower quality and performance than the original material. This has led to large-scale environmental accumulation, contributing to one of the most significant global environmental challenges, plastic pollution. Hence, conventional recycling methods alone are insufficient to address these challenges, highlighting the need for more sustainable alternatives. One possible solution is biotechnological recycling, which utilises microorganisms and enzymes, proteins that catalyse biochemical reactions, to break down plastic polymers into smaller molecules. These molecules can potentially be upcycled and reused in the production of new materials, contributing to a more sustainable and circular plastic economy. Therefore, this study investigated the chemoenzymatic modification of the major types of PE, including high-density polyethylene (HDPE), low-density polyethylene (LDPE), low-density polyethylene containing antioxidants (LDPEa) and linear low-density polyethylene (LLDPE). The aim was to optimise the treatment by combining two distinct chemical oxidation methods with enzymatic treatment and to identify the potential degradation products formed during the reaction. The chemical pretreatments used were potassium permanganate oxidation and Fenton oxidation. To further enhance the oxidation process, Fenton oxidation was also combined with UVC irradiation. After these treatments, new oxygen containing functional groups were introduced to the polymer backbone, indicating that oxidation had successfully occurred. The PE polymers were then treated with laccase, an enzyme known to oxidise PE. Laccase enzymes from both fungal and bacterial sources were used to investigate how the enzyme source influences the reaction. Following the enzymatic treatment, multiple oxygenated functional groups were introduced to the polymer backbone. Microscopy revealed clear surface modifications, including cracks and particle accumulations, while elemental analysis confirmed the presence of oxygen and nitrogen on the surface. In addition, the melting temperature and crystallinity generally decreased, indicating structural changes in the material. The study revealed that LDPE and LDPEa were most susceptible to modification. Furthermore, the bacterial laccase worked with both pretreatments but performed best with permanganate, while the fungal laccase worked better with Fenton chemistry. Combining UVC with Fenton further enhanced the chemoenzymatic oxidation. The released oxidative degradation products could be detected and identified, revealing that the bacterial laccase predominantly produced longer fatty acids. In contrast, the fungal laccase generated a broader range of products, from shorter hydroxy acids, polyoxidised intermediates and longer fatty acids. These products have the potential to be converted into high value chemicals and building blocks. For example, in the synthesis of biodegradable bioplastics, medical devices or cosmetics. Overall, this study further supports the potential of biotechnological recycling as a more sustainable alternative to conventional methods, transforming waste that causes significant environmental issues into valuable, sustainable resources.

Table of Contents

1. Introduction

High durability, light weight and low cost are only a few of the properties that make plastics an essential and irreplaceable component in many applications. However, this global plastic dependency has ultimately resulted in an annual production exceeding 400 million tons (Zhang, et al, 2025). The material's versatility is evident from its widespread use in industries such as textiles, construction, medicine and packaging (Zandieh, et al, 2023). As illustrated in Figure 1, packaging solutions alone account for the largest share of global plastic production and represent the major contributor to plastic waste generation. While these products are essential for reducing food waste and making fresh food more accessible, their single use nature generates significant amounts of plastic waste. Currently, only 14% of this waste is collected for recycling and the majority is mechanically downcycled into lower value products (Dokl, Copot, & Krajnc, 2024).

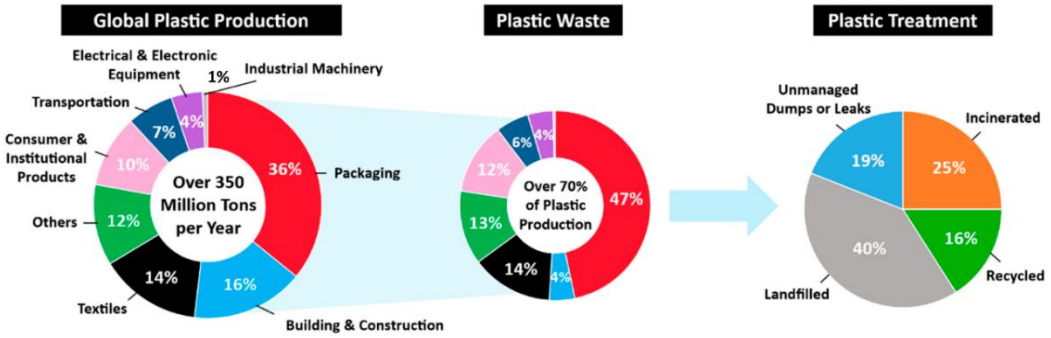

Figure 1: Statistics of global plastic production, plastic waste and treatment (Soong, Sobkowicz & Xie, 2022).

The very same properties that make plastics highly desirable in industrial applications cause challenges in their recyclability and end of life management. Their chemically inert nature, high molecular weight and hydrophobicity make them highly resistant to degradation (Temporiti, Nicola, Nielsen, & Tosi, 2022). Natural degradation can take up to several hundreds of years (Zandieh et al, 2023). The combination of the increased production and the inadequate waste management has led to one of the most significant global environmental challenges, plastic pollution (Temporiti, Nicola, Nielsen, & Tosi, 2022).

The extent of current plastic dependency and the resulting pollution clearly demonstrate that conventional chemical and mechanical recycling methods are insufficient. The main challenges with these methods include limited degradation efficiency, high energy consumption and significant environmental impact. These challenges emphasise the critical need for more sustainable alternatives, such as biotechnological degradation.

Therefore, the aim of this study is to investigate chemoenzymatic modification of four specific polyolefins: LDPE, LDPEa (LDPE containing antioxidants), LLDPE and HDPE. The overall process will be optimised by evaluating two distinct chemical pretreatments, $KMnO_4$/HCl and Fenton oxidation, followed by enzymatic treatment using laccase in a TEMPO-mediated system. In addition, Fenton oxidation will be combined with UVC irradiation to evaluate potential synergistic effect. To investigate the impact of the enzyme source, laccases from both bacterial (*Bacillus subtilis*, L.CotA) and fungal (*Myceliophthora thermophila*, L.MT) sources will be used. Finally, the chemoenzymatic treatments will be evaluated based on the potential upcycling of the resulting degradation products.

2. Scientific Background

2.1 Polyolefins

Polyolefins account for nearly half of the global plastic production, making them the most widely produced type of plastic. Their polymer backbone consists entirely of saturated C-C and C-H bonds which makes them exceptionally stable and difficult to degrade. In addition, the hydrocarbon backbone provides chemically inertness, mechanical flexibility, resistance to moisture and cost effectiveness, making them especially suitable for packaging applications (Charitopoulou & Achilias, 2026).

The two main types of polyolefins are polyethylene (PE) or polypropylene (PP), which are produced through polymerisation of ethylene and propylene monomers, respectively. These monomers are primarily derived from petroleum oil and natural gas. There are different types of PE, including low density polyethylene (LDPE), linear low-density polyethylene (LLDPE) and high-density polyethylene (HDPE) (Charitopoulou & Achilias, 2026), the different structures are presented in Figure 2.

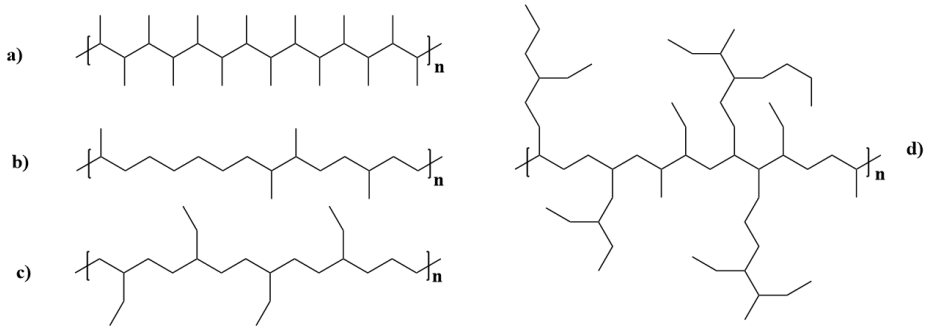

Figure 2: The chemical structure of PP (a), HDPE (b), LLDPE (c) and LDPE (d).

The molecular branching, density and degree of crystallinity vary significantly between the polyolefins, resulting in distinct mechanical and chemical properties. Polymers with a higher degree of crystallinity are stronger, stiffer and are inherently more resistant to degradation. In contrast, polymers with more branching are softer, more flexible and easier to degrade (Zhang, Ding, & Yuan, 2022).

Typically, LDPE and LLDPE have a lower degree of crystallinity and melting temperature compared to HDPE and PP. Due to their lower crystallinity, LDPE and LLDPE are highly flexible materials mainly used in packaging solutions. Specifically, LDPE is predominantly used in carrier bags, coatings and toys, whereas LLDPE is more commonly used in stretch and industrial packaging films and thin-walled containers. In contrast, the high crystallinity of HDPE makes it more rigid and mechanically robust, making it suitable for plastic membranes, structural components, protective headgear, pipes and transport containers. Lastly, PP exhibits excellent tensile strength and resistance to acids, bases and solvents making it suitable for yoghurt containers, pipes, carpet fibres and furniture (Charitopoulou & Achilias, 2026).

2.2 Conventional Plastic Recycling

Currently, plastic waste is mainly mechanically recycled, in which the waste is physically separated, sorted, melted and reprocessed. This straightforward method is widely used due to its ability to handle large amounts of waste. However, it is generally considered a form of downcycling, as the resulting products exhibit lower mechanical properties compared to the virgin material (Hadigheh, et al, 2025). These properties decline with each reprocessing cycle, essentially only delaying the final disposal of the material. Another challenge is its inability to process contaminated or multilayered waste, often leading to incineration (Lomwongsopon, et al, 2025), which releases toxic gases and pollutants further contributing to environmental contamination (Hadigheh, et al, 2025).

Chemical recycling emerged as a solution to manage various types of plastic waste and produce degradation products of higher value. The most widely studied method is pyrolysis, in which plastic waste is heated to high temperatures in an anaerobic environment, depolymerising it into monomers. The degradation products can then be converted into fuels or chemical feedstocks. The main drawback of chemical recycling is the high energy consumption required for effective degradation, which inherently increases greenhouse gas emissions (Hadigheh, et al, 2025). The energy consumption can be reduced by using a catalyst, which enable degradation at lower temperatures and shorter residence times while also increasing the selectivity of the degradation products. However, the current lack of highly efficient catalysts limits the scalability of chemical recycling (Charitopoulou & Achilias, 2026).

2.3 Biological Plastic Recycling

Biotechnological recycling uses enzymes and microorganisms to degrade plastic waste. This method offers a more sustainable approach because it operates under milder conditions, does not require the use of toxic chemicals and can process mixed post-consumer waste. In addition, degradation and upcycling can be integrated into a single process, further distinguishing it from conventional recycling methods (Lee, et al, 2023).

The first step in the biodegradation process is oxidation of the hydrophobic hydrocarbon backbone through the introduction of oxidative functional groups. The most common oxidation methods include UV irradiation, hydroxyl or sulphate radical based oxidation, Fenton reactions, strong acid treatments and oxygen plasma treatment. Following oxidation, microbial enzymes attach to the surface and metabolise the oxidative functional groups, initiating the degradation of the polymer backbone (Lomwongsopon, et al, 2025). This process subsequently leads to polymer fragmentation, during which oxidative enzymes cleave the carbon chain into smaller fragments, releasing intermediate products such as long-chain aliphatic compounds (Zhang, Ding, & Yuan, 2022).

Subsequently, the enzymes generate additional intermediate compounds that facilitate cellular assimilation. Once assimilated, these compounds serve as carbon sources for the microbial cells and are further metabolised into water and carbon dioxide or methane, thereby completing the mineralisation process. In addition to enzymatic degradation, the microbes can grow on the polymer surface, leading to the formation of cracks and the enlargement of pores (Temporiti, Nicola, Nielsen, & Tosi, 2022). The overall degradation process is summarised in Figure 3.

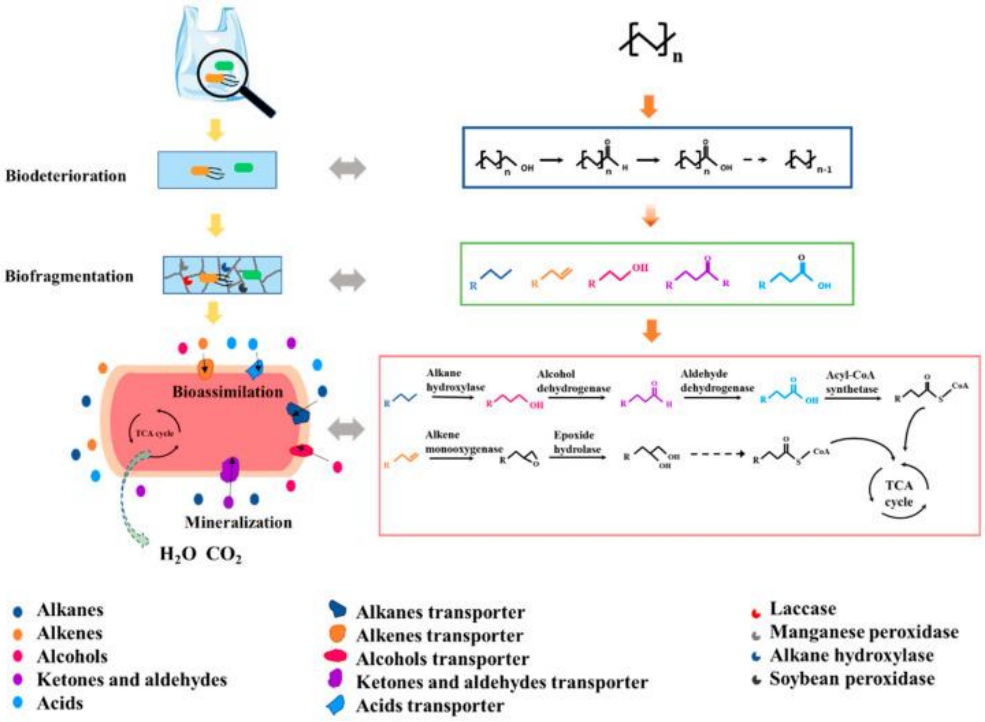

Figure 3: Overview of the biodegradation process of plastic waste (Zang, Ding & Yuan, 2022).

The main drawbacks of biotechnological recycling include prolonged reaction times and low overall degradation efficiency. These limitations are largely influenced by the type of microorganism employed, the operating conditions and the properties of the plastic waste. Optimising these parameters could significantly enhance the efficiency and practical applicability of the process (Hadigheh, et al, 2025). Additionally, the high specificity of enzymes limits their applicability in complex real-world applications. A limited mechanistic understanding of the interactions between the enzyme and substrate hinders the design of more versatile and effective enzymes. Given that the rate determining step is the polymer depolymerisation, enzymatic attack and chain scission are frequently targeted to improve the biological pathways involved in plastic degradation (Ding, et al, 2026).

2.4 Laccases

Enzymes are proteins that function as catalysts in biological systems (Zandieh, et al, 2023). One enzyme class proven to effectively degrade polyolefins in lab scale is laccase, a multicopper monomeric glycoprotein that belongs to the blue copper oxidase family. Laccase effectively oxidises compounds by using oxygen as an electron acceptor and reducing it into water. As an extracellular enzyme, its non-specific nature allows it to degrade polymers by overcoming their inherent hydrophobicity. Industrial applications of laccases include delignification, pulp bleaching and bioremediation for the removal of toxic compounds (Temporiti, Nicola, Nielsen, & Tosi, 2022).

The current understanding of the enzymatic degradation mechanism is that laccase initially target reactive surface groups before penetrating deeper into the polymer matrix, eventually leading to molecular breakdown. For PE, this process involves cleavage of the main chain hydrocarbon bonds and progressive chain oxidation, yielding small oxidative intermediates. However, the exact mechanism is still poorly understood, limiting the practical applications, especially regarding the substrate recognition, bond cleavage and formation of intermediate products (Ding, et al, 2026).

Recent studies have demonstrated that degradation efficiency can be significantly enhanced through laccase mediated systems, where laccase enzyme catalyses the formation of reactive mediator radicals that further attack the polymer chain (Ding, et al, 2026). Common redox mediators for PE degradation include 1-hydroxybenzotriazole (HBT), 2,2-azino-bis(3-ethylbenzothiazoline-6-sulfonicacid) ABTS and (2,2,6,6-tetramethyl-1-piperidinyl)oxyl (TEMPO) (Zandieh, et al, 2023). Redox mediators essentially function as an electron carrier between the enzyme and the substrate. First, laccase oxidises the mediator into a stable radical or cation, which then diffuses and oxidises the target substrate, illustrated in Figure 4. This mechanism effectively broadens the enzyme's substrate range and enhances the overall reaction rates (Younus, Khan, Khan, & Alhumaydhi, 2025).

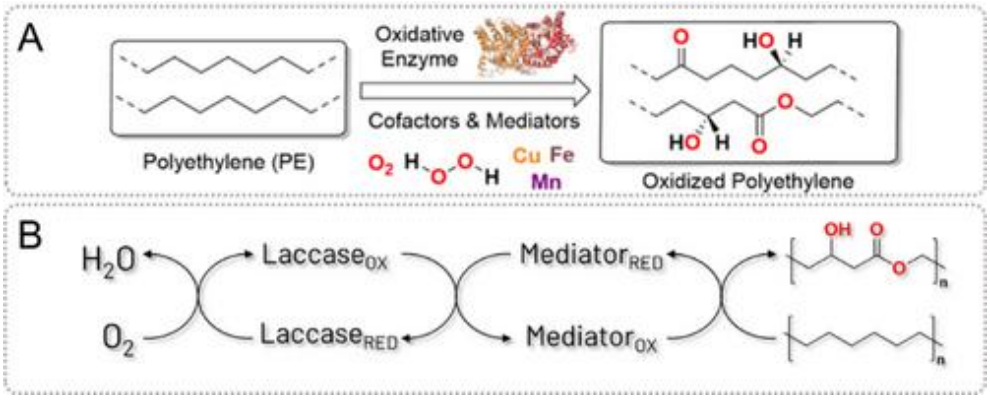

Figure 4: Overview of a) enzymatic degradation of PE and b) PE oxidation via a laccase mediator system (Zandieh et al, 2023).

Laccase is primarily expressed from fungal and bacterial sources, which directly impacts their catalytic stability, redox potential and potential application. While fungal laccases have a higher redox potential, they are more sensitive to extreme environments with their optimal conditions between pH 3.5 to 5.5 and 30 ℃ to 55 ℃ (Li, Tian, Ren, Wang, & Liu, 2025). Conversely, bacterial laccases are stable at higher temperatures, broader pH range and less sensitive to solvent conditions. From a production perspective, it's faster, easier and more cost effective to express Laccase from bacteria compared to fungi, primarily due to the slower growth rate of fungi. Additionally, large-scale production of fungal laccase generates large amounts of biomass which are difficult to dispose of. Therefore, bacterial laccase has gained more attention in industrial applications (Panwar, Lzaod, & Dutta, 2023)**.**

L.CotA is one of the most extensively studied bacterial laccases. It exhibits high thermal and alkaline stability, with an optimal temperature range between 60 ℃ to 80 ℃ and an optimal pH range between 4 and 8.5. Potential industrial applications include biochemical pulping for lignin degradation and treatment of textile dyes. The purified enzyme has a molecular weight of approximately 65 kDa. The addition of copper salt during the expression step essential for enzyme activity (Hou et al, 2024). One study degraded UV treated PE using L.CotA in a mediator system. The treatment resulted in surface etching, fragmentation and cracking, as well as formation of oxygenated functional groups and oxygen containing degradation products such as aldehydes, ketones and alcohols (Yao, et al, 2022). In comparison, L.MT is a widely used commercial fungal laccase with a molecular weight of 61 kDa. It has demonstrated high efficiency and selectivity in industrial applications, including paper bleaching, degradation of dyes and antibiotics as well as tissue whitening. However, the enzyme exhibits limited resistance to organic solvents and has reduced thermal stability (García, et al, 2024).

2.5 Recent Progress in Polyolefin Degradation

Some studies on biotechnological recycling of polyolefins have attempted degradation without the oxidation pretreatment step. One potential approach was to construct a multienzyme complex system, which offered high efficiency, mature ester hydrolases, and fully mineralised products. The main limitations were the need for enzyme modification and the design of the Baeyer-Villiger reaction. Another potential approach was to use enzymes that could degrade polyolefins directly by generating reactive action sites. Reported examples of these enzymes include Demetra and Ceres sourced from wax worm saliva and Catalase-peroxidase from the intestines of insects (Kong, et al, 2024).

Additionally, one study on biodegradation of HDPE microplastic used the fungal strain *Aspergillus flavus*, which was isolated from the gut of the wax moth *Galleria mellonella*. This strain successfully depolymerised HDPE and produced lower molecular weight products after 28 days of incubation. *A. flavus* action could be attributed to its capacity to produce laccases and laccase-like multicopper oxidases (Temporiti, Nicola, Nielsen, & Tosi, 2022).

Similar results have been observed in other microorganisms, including *Alternaria alternata* FB1, *Aneurinibacillus*, *Brevibacillus*, *Pseudomonas vibrio* and *Aspergillus niger.* Using *Alternaria alternata* FB1 in basic medium resulted in formation of C=O bonds, the release of diglycolamine degradation products and a decrease in crystallinity from 63 % to 52 %. Using *Aneurinibacillus* or *Brevibacillus* resulted in a 37 % to 45 % weight loss, formation of C=O bonds and degradation products like tridecanoic acid and octadecanoic acid after 140 days at 50 °C. Lastly, *Pseudomonas Vibrio* and *Aspergillus niger* combined with starch resulted in 40 % weight loss, formation of C=O and O-H bonds and hydrocarbon degradation products ranging from $C_{10}H_{22}$ to $C_{31}H_{64}$ after 175 days at 30 °C (Lee, et al, 2023).

On commercial scale, the company Entzimatiko offers enzyme complexes derived from fungal sources that are capable of depolymerising polyolefins without a chemical pretreatment step. Through nanoencapsulation, the enzymes can attach to the hydrophobic polyolefin surface. Once attached, these multienzymes break down the polymer matrix more efficiently than individual enzymes. The process operates as a simple one-pot system without specific pH requirements. It is dived into four main operations: enzymatic degradation, gravimetric deposition, monomer extraction via centrifugation and recovery, ultimately resulting in a cyclic monomer to monomer process (Entzimatiko, 2026).

To enhance the degradation of mixed plastic waste, one study combined UVC-Fenton oxidation with a mixed microbial consortium. This improved the degradation of PE and PP by 4.3 and 27 times. The mixed microbial culture was effective on mixed plastic due to its high substrate utilisation, versatility from synergistic interactions, increased tolerance to degradation products and distribution of metabolic burden among the different species. However, proper pretreatment was still required to overcome the inherently slow degradation of polyolefins (Lomwongsopon, et al, 2025).

Lastly, one study on chemoenzymatic degradation of PE used mCPBA and ultrasonication as the pretreatment step. Followed by enzymatic degradation using a multi-enzyme complex of catalase-peroxidase, alcohol dehydrogenase, Baeyer Villiger monooxygenase and lipase. The identified degradation products where 7-hydroxyheptanoic acid, 9-hydroxynonanoic acid, 11-hydroxyundecanoic acid, 14-hydroxytetradecanoic acid, 16-hydroxyhexadecanoic acid, sebacic acid, undecanedioic acid, dodecanedioic acid and tridecanedioic acid (Oiffer, et al, 2024).

3. Materials and Methods

3.1 Materials

LDPE, LDPEa, HDPE and LLDPE films with a thickness of 100 µm were provided by Tetra Pak. Fungal laccase from *Myceliophthora thermophila* (L.MT) was obtained from Novozymes (Denmark), Hydrochloric acid (HCl, 37 %) from Honeywell Fluka (Austria), Ethanol (>99.5 %) from SOLVECO (Sweden), IPTG from Takara (Japan), N-Methyl-N-(trimethylsilyl) heptafluorobutylamide (MSHFBA, >95 %) from MACHEREY-NAGEL (Germany), Tris base from Alfa Aesar (Germany) and TEMPO from BioSynth (Slovakia). Ampicillin (Belgium) and Sodium Chloride (NaCl, >99.5 %, UK) from Fisher. ABTS (98 %, China) and Citric acid (>99 %, Germany) from Merck. Copper Sulfate ($CuSO_4$, >99 %, India), Dichloromethane (DCM, 99.8 %, France), Hydrogen Peroxide (H_2O_2, 30 %), Sodium Citrate dihydrate (>99 %, Austria), Sulfuric acid (H_2SO_4, USA), Tryptone (USA), Yeast Extract (France) and Iron (II) Sulphate Heptahydrate ($FeSO_4 \cdot 7H_2O$) from Sigma Aldrich. Imidazole (Germany) and Potassium Permanganate ($KMnO_4$, 98 %, Belgium) from Thermoscientific. All chemicals were used without further purification.

3.2 Methods

An overview of the chemoenzymatic process used in this study is presented in Figure 5. Detailed protocols are listed below.

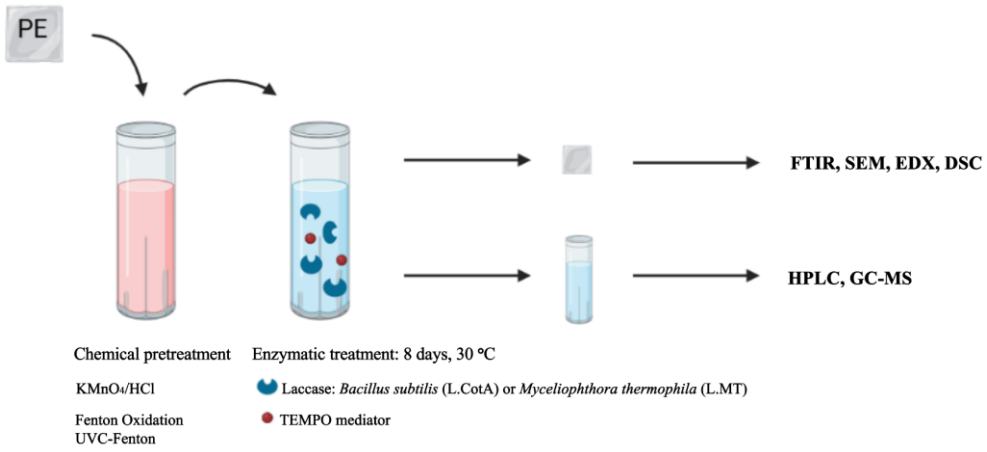

Figure 5: Schematic overview of the chemoenzymatic process, including chemical pretreatment, enzymatic treatment and analytical characterisation techniques for solid and liquid samples. The image was created with BioRender.com.

3.2.1 Expression & Purification of Laccase CotA

To express bacterial L.CotA, a preculture with *E. coli* BL21 glycerol stock supplemented with 100 µl/ml ampicillin was added to LB agar medium (10 g/l Tryptone, 10 g/l NaCl, 5 g/l yeast) and incubated overnight at 37 °C and 200 rpm. Following incubation, the culture was grown in LB medium supplemented with 100 µg/ml of ampicillin until OD_{600} reached 0.7. The protein was then expressed by adding 0.4 mM $CuSO_4$, and 0.5 mM IPTG followed by incubation at 16 °C, 100 rpm for 24 hours (Zadeh, 2024).

The cells were harvested by centrifugation at 4 °C, 4500 rpm for 30 min. The resulting pellet was resuspended in binding buffer (50 mM Tris base, 0.5 M NaCl, 20 mM imidazole, pH 8) and lysed

via sonication at 30/30 pulses at 30 % amp for 5 min. The lysed protein was separated from the *E. coli* by centrifugation at 4 ℃, 13200 rpm for 15 min. The supernatant was then filtered through a 0.45 µm syringe filter and purified using ÄKTA start chromatography system equipped with a 1 ml HisTrap column and elution buffer (50 mM Tris base, 0.5 M NaCl, 0.5 M imidazole, pH 8) (Zadeh, 2024).

The purified enzyme solution was analysed with sodium dodecyl sulphate polyacrylamide gel electrophoresis (SDS-page, Mini-PROTEIN TGX Stain-Free Gel, Bio-Rad) and the concentration was determined using a ThermoScientific Nanodrop 1000 spectrophotometer. The final L.CotA solution was stored at 4 ℃.

3.2.2 Enzyme Activity Assay

The enzyme activity of L.CotA was measured against 5 mM ABTS in 0.1 M citrate buffer with pH 5 using a BioTek Synergy H1 microplate reader. The reaction was monitored at 420 nm in one-minute intervals for 8 min, (Zadeh, 2024). The activity was calculated using Beer-Lamberts law:

$$A = \varepsilon \cdot l \cdot c$$

where A is the absorbance, ε is the molar absorptivity coefficient of ABTS radical, l is the path length and c is the concentration.

3.2.3 Chemical Pretreatment

To enhance surface oxidation and enzymatic susceptibility, 10 mg/ml PE films were subjected to two distinct chemical pretreatments, $KMnO_4$/HCl and Fenton oxidation. In addition to this, LDPE films were treated with a combination of UVC irradiation and Fenton oxidation.

3.2.3.1 $KMnO_4$/HCl

Polymer films were immersed in 1ml of 0.25M $KMnO_4$/0.1M HCl solution, at 60℃ and 400rpm for 24h. Following treatment, the films were washed with 12M HCl to remove any surface residue and reaction by products (Zadeh, 2024). To investigate the temperature dependency of the reaction, LDPEa, LLDPE and HDPE films were treated with the same protocol but at 80℃.

3.2.3.2 Fenton Oxidation

Two different Fenton conditions were evaluated. The first method was adapted from a Fenton oxidation of lignin protocol (Jeong, et al, 2018). The polymer films were immersed in 0.75 ml of 10 M H_2O_2, at 30 ℃ and 400 rpm for 2 hours. 12.5 mg of $FeSO_4 \bullet 7H_2O$ was dissolved in 0.25 ml distilled water and 50 µl was added to the reaction every 10 min, total 5 doses. To investigate how the iron concentration affected the oxidation, the same protocol was used but with 25 mg of $FeSO_4 \bullet 7H_2O$.

The second protocol used general optimal conditions for Fenton oxidation, which was a pH of around 3 to 5 and a Fe^{2+}:H_2O_2 ratio of 1:10 (Fentons Reagent General Chemistry Using H_2O_2, n.d). The polymer films were immersed in 0.05 M $FeSO_4 \bullet 7H_2O$/0.5 M H_2O_2 solution at 50 ℃ and 200 rpm for 15 hours, with pH adjusted to 3 using HCl. After 15 hours, a small dose of 10 M H_2O_2 was added and the reaction ran for an additional hour.

Following treatment, the films were immersed in 0.1 M HCl until transparent, then rinsed with water and 70 % ethanol to remove any remaining surface residue.

3.2.3.3 UVC

LDPE films were exposed to UVC irradiation at a wavelength of 254 nm for 60 min in a closed, protective UV chamber.

3.2.4 Enzymatic Treatment

The PE films were subjected to enzymatic treatment using fungal (L.MT) and bacterial (L.CotA) laccases. The films were immersed in a 0.1 M citrate buffer (pH 5) containing 5 mM TEMPO. The reactions were carried out on a heating block at 30 °C and 400 rpm for 8 days. Fresh enzyme was added every 24 hours to maintain catalytic activity. For the fungal Laccase, 150 µl of concentrated L.MT was added, while for the bacterial Laccase, L.CotA was added to a final concentration of 4.25 µM. The total reaction volume was kept constant at 1 ml. (Zadeh, 2024).

3.3 Analytical Methods

3.3.1 Fourier Transform Infrared Spectroscopy (FTIR)

To see changes in the functional groups, the polymer films were analysed with Thermoscientific Nicolet iS5 using the ZnSe crystal, performing 16 scans in the wavenumber range of 4000 cm^{-1} – 500 cm^{-1} and a total reflection mode, T %, transmission. Sample preparation included washing the films with water followed by 70 % ethanol and then air dried to remove any surface residues that could interfere with the measurements. The carbonyl index (CI) was calculated with the following equation:

$$CI = \frac{A_{Carbonyl\ Peak}}{A_{Methylene\ Peak}}$$

Where $A_{Carbonyl\ Peak}$ is the area in the range of 1840 cm^{-1} – 1510 cm^{-1} and the $A_{Methylene\ Peak}$ is the area in the range of 1495 cm^{-1} - 1427 cm^{-1} (Lomwongsopon, et al, 2025).

3.3.2 High Performance Liquid Chromatography (HPLC)

To precipitate and remove proteins from the reaction mixture, a small amount of 0.01 M H_2SO_4 was added and the mixture was kept at 4 ℃ for 15 min. Then, it was centrifuged at 12000 rpm for 5 min. The HPLC analysis was performed using an LC4000 system (JASCO, Japan), equipped with an Aminex HPX-87H chromatographic column (100 x 7.8 mm). The mobile phase was 0.5 mM H_2SO_4, with a flow rate of 0.6 ml/min and an oven temperature of 65 ℃. Detection was performed by using both a UV detector at 254 nm and an RI detector.

3.3.3 Gas Chromatography–Mass Spectrometry (GC-MS)

Potential degradation products were extracted by mixing 200 µl of the reaction mixture with 200 µl of dichloromethane (DCM) at room temperature for 15 min. The extracted products were derivatised by adding 50 µl of N-Methyl-N-(trimethylsilyl) heptafluorobutylamide (MSHFBA) and incubating

at room temperature for 1 hour. The GC-MS analysis was performed using a Thermoscientific TRACE 1300 Gas Chromatograph coupled to an ISQ 7610 Mass Spectrophotometer. Separations were performed on an Ultra inert GC column 15m x 0.25 mm, 0.25 μm with Helium as the carrier gas. Injection was performed split mode with the injector temperature at 250 °C. The oven temperature program held at 80 °C for 3 min, followed by a 15 °C/min ramp up to 275 °C. The mass spectrometer operated in EI scan mode over a mass range of 40 - 400 m/z at 70 eV.

3.3.4 Differential Scanning Calorimetry (DSC)

Thermal analysis of PE films were performed using a Mettler Toledo DSC5+ instrument in power compensation mode. All measurements were done under nitrogen gas. The samples were studied with a heating and cooling rate of 10 ℃/min under nitrogen. The sequence consisted of a heating ramp from 35 to 180 ℃ with a 10 min hold at 180 ℃, followed by a cooling ramp to 0 ℃ with a 3 min hold at 0 ℃ and final a heating ramp to 190 ℃. A total of 8 samples were analysed, included untreated LDPEa, LLDPE and HDPE films along with LDPEa treated with both chemical pretreatments combined with L.CotA, LLDPE treated with Fenton oxidation combined with both enzymes and HDPE treated with $KMnO_4$/HCl combined with L.CotA. The degree of crystallinity was calculated with the following equation:

$$X_c(\%) = \left(\frac{\Delta H_m}{\Delta H_m^\circ}\right) \times 100\%$$

Where ΔH_m is the measured melting enthalpy and ΔH_m° is the melting enthalpy of PE with 100% crystallinity, which is 293 J/g for PE (NETZSCH, 2026).

3.3.5 Scanning Electron Microscopy (SEM) & Energy Dispersive X-ray Spectroscopy (EDX)

To investigate modifications in the surface morphology, PE films before and after chemoenzymatic treatment were analysed using SEM at an acceleration voltage of 5 kV. Samples were mounted on brass SEM stubs using conductive adhesive tabs and coated with carbon prior to analysis. The SEM was coupled with EDX to investigate changes in chemical composition following treatment. For EDX analysis, the emission current was 20 μA and all images were acquired at x100 magnification. A total of 13 samples were analysed, including all four untreated films, all LDPE treatment conditions and the most optimal conditions for LDPEa, HDPE and LLDPE.

4. Results

4.1 Enzyme Expression & Purification

Two SDS-PAGE analyses were conducted to evaluate the expression and purification of L.CotA, see Figure 6. Both gels revealed distinct bands within the 60 - 70 kDa region, which is consistent with the reported molecular weight of 65 kDa for L.CotA (Hou, et al, 2024). However, due to differences in enzyme concentration, the bands appear quite different. The first gel had a much higher enzyme concentration, which overloaded the gel and produced smeared intense bands. In contrast, the second gel had a much lower enzyme concentration, resulting in weaker bands.

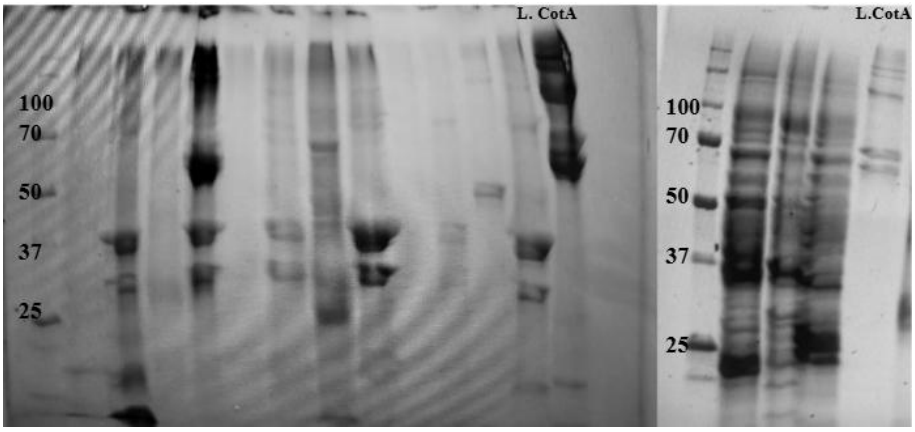

Figure 6: SDS-PAGE of purified Laccase expressed from Bacillus subtilis (L.CotA), high concentration (left), lower concentration (right). Only the lanes labelled "L.CotA" belong to this project, the other lanes contain unrelated samples from another project.

The enzyme concentration was quantified using Nanodrop spectrophotometer. The protocol demonstrated high reproducibility, as 1 g of harvested cell pellet consistently resulted in a purified enzyme concentration of approximately 1 mg/ml. To evaluate the catalytic activity of the purified L.CotA, an ABTS oxidation assay was performed. After adding L.CotA, the reaction mixture quickly turned green, which is characteristic for the formation of ABTS radical (More, et al, 2011). The specific activity of the purified laccase was calculated to be 1.02 U/mg using Beer-Lamberts law:

$$c = \frac{A}{\varepsilon \cdot l} = \frac{0.276}{36\,000\ M^{-1}cm^{-1} \cdot 0.3cm} \times 10^3 = 0.0256\ mM$$

$$Specific\ activity = \frac{\Delta c/\Delta t}{[L.CotA]_{Assay}} = \frac{0.0256\ mM\ /\ 1\ min}{0.025\ mg/ml} = 1.02\ U/mg$$

The observed colour change, together with the molecular weight confirmed by SDS-page analysis and the calculated specific activity collectively verified successful expression and purification of L.CotA.

4.2 Oxidative Modification of the Polymer Backbone

FTIR analysis of PE films treated with $KMnO_4$/HCl at 60 °C for 24 hours revealed a distinct new peak at 1717 cm^{-1}, Figure 7. This peak corresponds to carbonyl (C=O) stretching, which confirms successful oxidation of the polymer backbone. Increasing the reaction temperature to 80 °C resulted in a minimal increase in the intensity carbonyl peak compared to 60 °C.

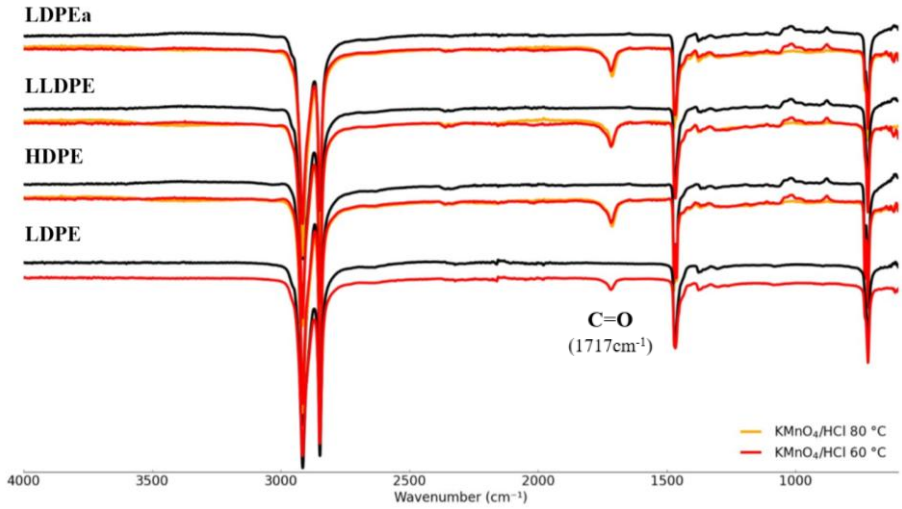

Figure 7: FTIR spectra of LDPEa, LLDPE, HDPE and LDPE films before and after oxidation treatment with $KMnO_4$/HCl. For each polymer, the black curve represents the untreated film, while the red curve represents the film after treatment at 60°C and the orange curve represents the film after treatment at 80°C.

Applying reaction conditions adapted from lignin oxidation on PE films did not result in any observable changes, except for an increase of the C-O stretching region at 1083 cm^{-1} when using a lower iron concentration. In contrast, implementing more optimised Fenton conditions, combined with higher temperature, longer reaction time and the stepwise dosing strategy from the lignin study revealed multiple peaks. These include carbonyl (C=O) stretching at 1717 cm^{-1}, C-O stretching at 1083 cm^{-1}, hydroxyl (O-H) stretching at 3353 cm^{-1} and unsaturated alkene (C=C) stretching at 1622 cm^{-1}, shown in Figure 8.

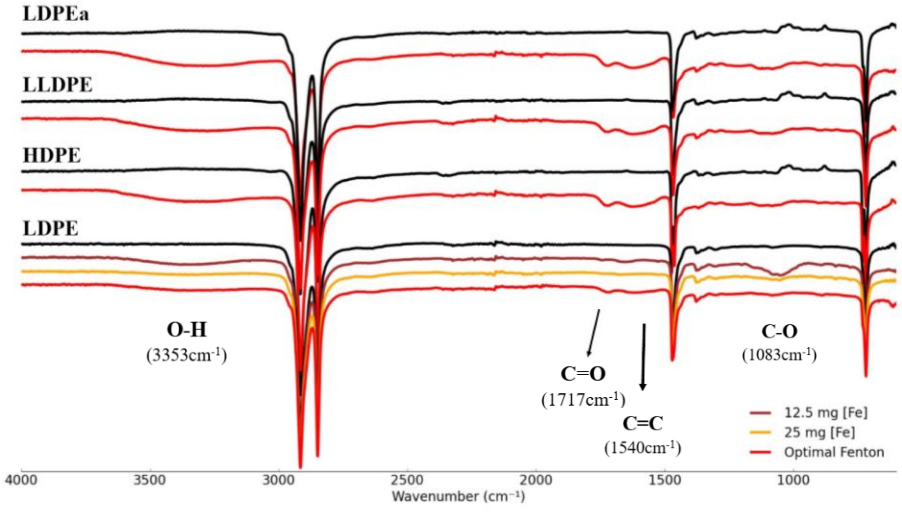

Figure 8: FTIR spectra of LDPEa, LLDPE, HDPE and LDPE films before and after Fenton oxidation. For each polymer, the black curve represents the untreated film and the red curve represents the film treated with optimal Fenton conditions. For LDPE, the brown curve represent treatment with lower iron concentration and orange curve represents treatment with higher iron concentration, selected based on conditions used in the lignin study.

FTIR analysis of the PE films after 8-days of enzymatic treatment revealed substantial structural modifications to the polymer backbone, see Figure 9. These modifications include carbonyl (C=O)

stretching at 1717 cm^{-1}, C-O stretching at 1083 cm^{-1}, hydroxyl (O-H) stretching at 3353 cm^{-1} and unsaturated alkene (C=C) stretching at 1622 cm^{-1}. See Appendix Figures A1-A3 for the corresponding LDPEa, LLDPE and HDPE chemoenzymatic spectra. For untreated LDPE, enzyme treatment resulted in minor modifications within the carbonyl regions. However, treatment with L.CotA exhibited more pronounced modifications compared to L.MT. In contrast, L.CotA treatment of untreated LDPEa, LLDPE and HDPE revealed distinct spectral changes in both the carbonyl (C=O) and unsaturated (C=C) regions. Combining chemical and enzymatic treatments significantly increased oxidation of the polymer backbone. Both $KMnO_4$/HCl and Fenton pretreatments enhanced the peak intensity of oxygen containing functional groups.

Chemoenzymatic treatment with L.CotA resulted in more pronounced modifications of the polymer backbone compared to L.MT. The most intense oxygen containing peaks were observed for $KMnO_4$/HCl coupled with L.CotA across all films except for LLDPE, where Fenton oxidation combined with L.MT exhibited slightly more intense oxidation of the polymer backbone.

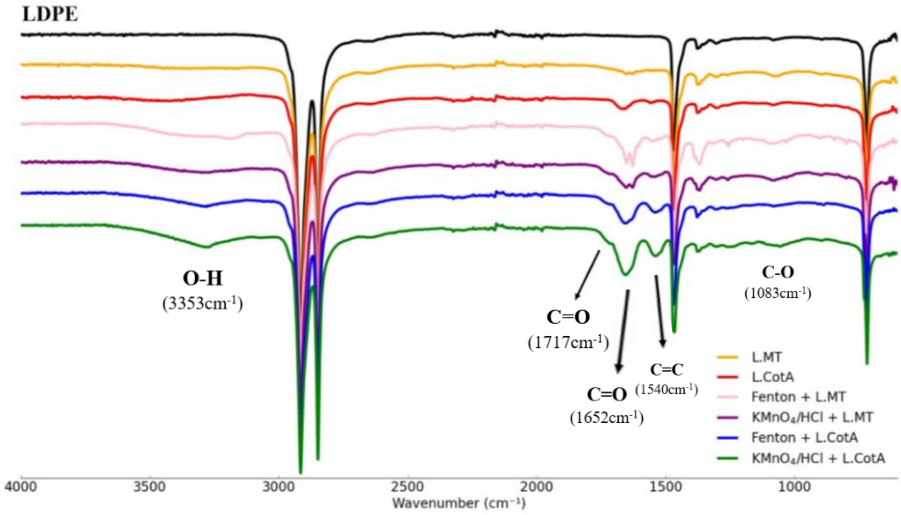

Figure 9: FTIR spectra of LDPE films following chemoenzymatic treatment. The black curve corresponds to the untreaded film, while the orange (L.MT) and red (L.CotA) curves correspond to films after enzymatic treatment alone. The pink and purple curves correspond to films pretreated with Fenton oxidation and $KMnO_4$/HCl oxidation, respectively, followed by treatment with L.MT. The blue and green curves correspond to films pretreated with Fenton oxidation and $KMnO_4$/HCl oxidation, respectively, followed by treatment with L.CotA

Exposing LDPE to UVC irradiation for 1 hour resulted in minor changes in the C-O region. Following Fenton treatment, signals in the O-H, C=O and C-O regions increased, see Appendix A4. Enzymatic treatment of the UVC-Fenton treated LDPE further increased the peaks corresponding to the hydroxy and carbonyl functional groups. This trend was observed for both L.MT and L.CotA, although L.CotA exhibited slightly more pronounced oxidation of the polymer backbone, see Figure 10.

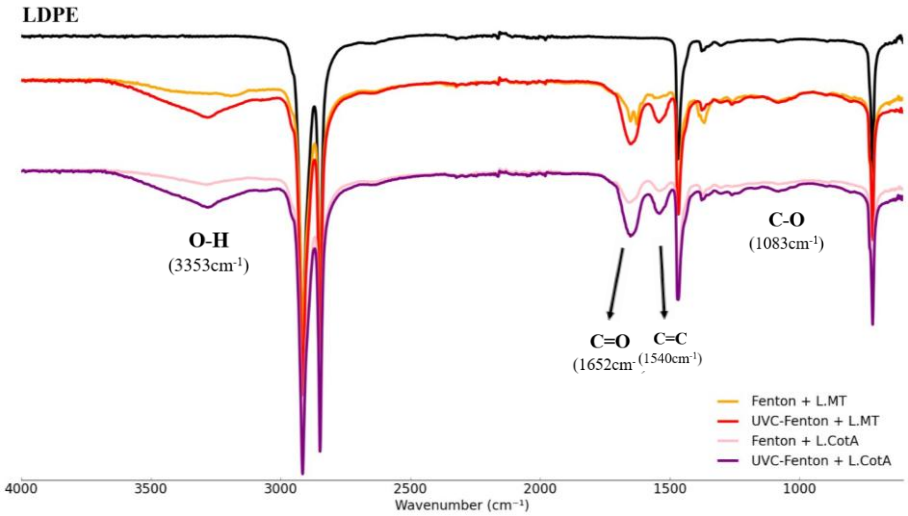

Figure 10: FTIR spectra of LDPE film following chemoenzymatic treatment: The black curve represents the untreated film. The orange and red curves correspond to films pretreated with Fenton oxidation and UVC-Fenton, respectively, followed by treatment with L.MT. The pink and purple curves correspond to films pretreated with Fenton oxidation and UVC-Fenton, respectively, followed by treatment with L.CotA.

To quantify the observations from FTIR analysis, the carbonyl indices (CI) were calculated following each chemical and enzymatic treatment, presented in Table 1. The calculated CI values supported the trends observed in the FTIR spectra, treatments that exhibited more pronounced carbonyl peaks naturally yielded high CI values, indicating a greater extent of oxidative modification of the polymer backbone.

A comparison of the CI values revealed that both pretreatments enhanced L.CotA was enhanced by both oxidation methods, with the highest values when coupled with $KMnO_4$/HCl. However, L.MT was much more effective when combined with Fenton oxidation. When L.MT was coupled with $KMnO_4$/HCl, the CI values were unexpectedly lower than those obtained after the individual treatments. Additionally, LDPE consistently exhibited lower CI values than LDPEa, LLDPE and HDPE following the individual chemical and enzymatic treatments. However, after chemoenzymatic treatment, the CI values for LDPE were generally among the highest observed. Overall, most chemoenzymatic treatment resulted in a higher CI value than those obtained from their individual treatments, indicating a synergistic effect between the chemical and enzymatic treatments.

Table 1: Calculated carbonyl index (CI) values after chemical and enzymatic treatments of LDPE, LDPEa, LLDPE and HDPE. CI values and respective error bars are based on three measurements.

PE	$KMnO_4$/HCl	Fenton	L.CotA	L. MT	$KMnO_4$/HCl +L.CotA	Fenton +L.CotA	$KMnO_4$/HCl + L.MT	Fenton + L.MT
LDPE	1.01±0.12	0.17±0.02	0.40±0.02	0.22±0.05	**2.33**±0.15	1.16±0.11	1.07±0.11	2.01±0.14
LDPEa	2.01±0.20	0.73±0.03	1.64±0.11	0.39±0.07	**2.50**±0.14	2.44±0.17	1.08±0.11	1.20±0.07
LLDPE	1.81±0.12	0.49±0.03	1.43±0.11	1.17±0.15	1.86±0.15	1.87±0.13	0.95±0.07	**1.94**±0.14
HDPE	1.55±0.15	0.43±0.02	1.43±0.09	1.13±0.13	**2.20**±0.17	1.62±0.13	0.76±0.05	1.50±0.10

This synergistic behaviour was particularly pronounced for the UVC-Fenton treatment, where the CI more than doubled after the initial chemical oxidation step and increased by factors of 2.3 and 1.23 following enzymatic treatment with L.CotA and L.MT respectively, shown in Table 2.

Table 2: Calculated carbonyl index (CI) values after UVC-Fenton oxidation and enzymatic treatment of LDPE. CI values and respective error bars are based on three measurements.

Treatment	UVC-Fenton	UVC-Fenton + L.CotA	UVC-Fenton + L.MT
CI	0.42±0.06	2.68±0.19	2.47±0.16

4.3 Morphological, Elemental & Thermal Modifications

SEM images of the untreated LDPE, HDPE and LDPEa control films revealed relatively smooth and homogeneous surfaces with only minor defects. Except for untreated LLDPE, which displayed more macro-scale fractures, see Appendix A5. Following chemoenzymatic treatment with $KMnO_4$/HCl and L.CotA, all PE films exhibited noticeable morphological modifications, including surface roughening, crack formation, localised etching formation and the accumulation of white clusters of particles, see Figures 12 and 13. Complementary images in Appendix A6-7 further support these findings.

Of all treated samples, LDPEa showed the most structural degradation, with deeper fractures, extensive cracking and more accumulated particles compared to the other films. In contrast, the surface of treated HDPE was still relatively smooth at x100 magnification. However, distinct clusters of accumulated particles was observed at x1000 magnification.

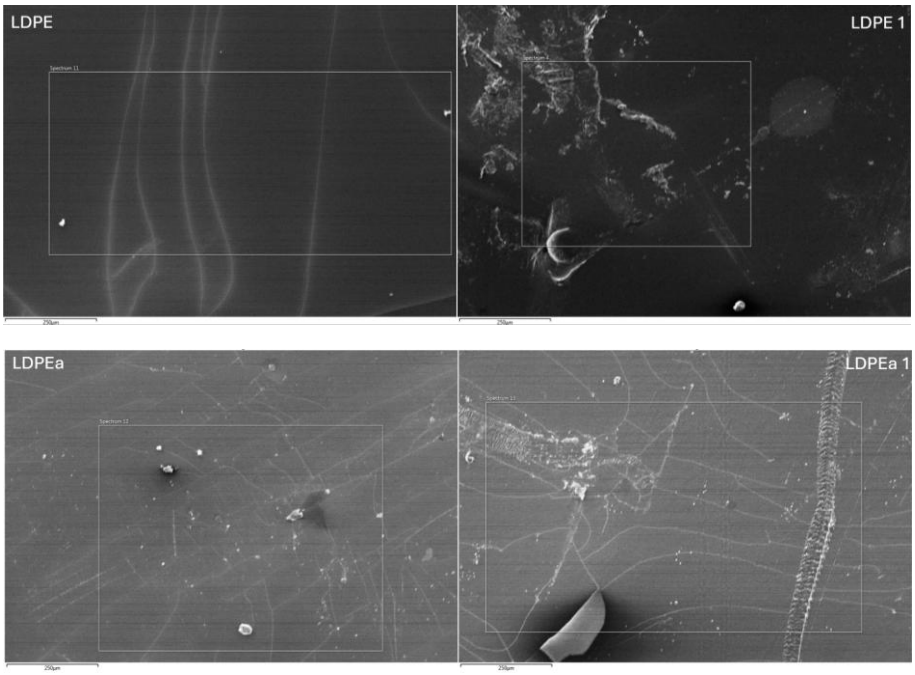

Figure 12: SEM images of untreated LDPE (top left), LDPE treated with $KMnO_4$/HCl followed by L.CotA (LDPE 1, top right), untreated LDPEa (bottom left) and LDPEa treated with $KMnO_4$/HCl followed by L.CotA (LDPEa 1, bottom right). The white boxes are the selected regions for EDX analysis, all images are taken at X100 magnification.

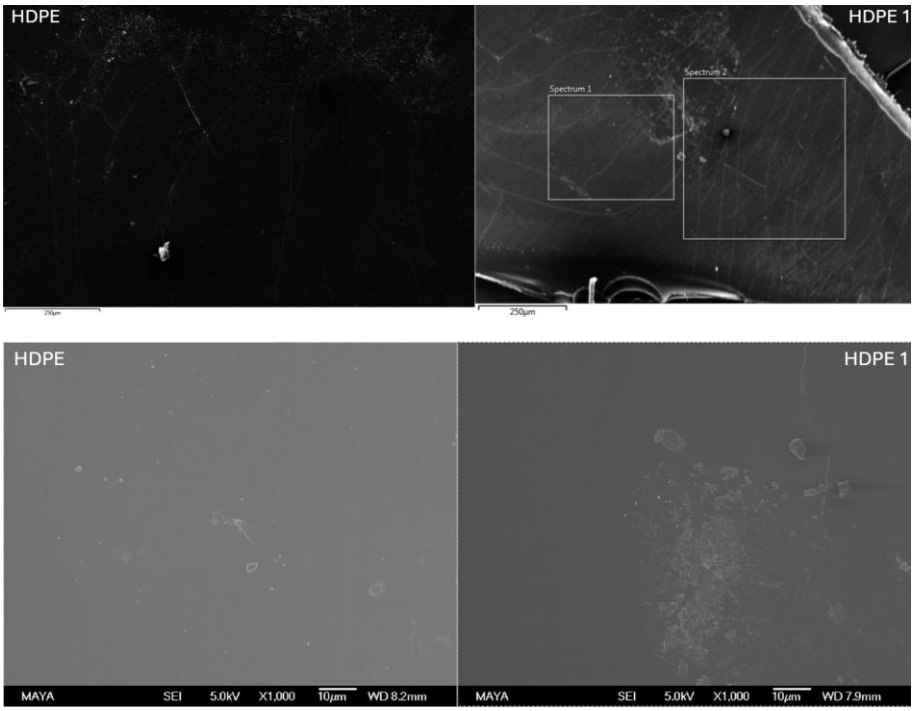

Figure 13: SEM images of untreated HDPE (x100, top left : x1000 bottom left) and HDPE treated with $KMnO_4$/HCl followed by L.CotA (HDPE 1, x100, top right : x1000 bottom right). The white boxes are the selected regions for EDX analysis.

To investigate changes in the surface elemental composition before and after chemoenzymatic treatment, SEM was coupled with EDX analysis, see Appendix A8 for an overlay of the recorded spectra. As shown in Figure 14, elemental mapping revealed a highly homogenous distribution of carbon, oxygen and nitrogen across the entire PE surface.

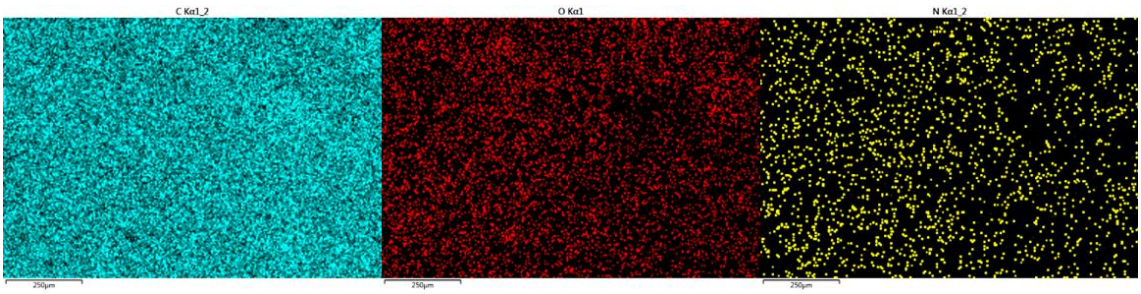

Figure 14: Elemental mapping of LDPE treated with UVC-Fenton followed by L.MT, showing distributions of carbon (blue), oxygen (red) and nitrogen (yellow)

As displayed in Figure 15, the untreated PE films had a baseline oxygen content of around 1.5 atom% and no detectable nitrogen. Following chemoenzymatic treatment, the atom% of oxygen and nitrogen increased for all films. Overall, the samples with the highest oxygen content had all been treated with L.CotA with LDPEa with the highest oxygen content at 8.36 atom%. For LDPE, the highest oxygen content was observed after $KMnO_4$/HCl + L.CotA and Fenton + L.MT treatments. In general, UVC-Fenton pretreatment increased the surface oxygen content. See Appendix A9 for the exact chemical compositions.

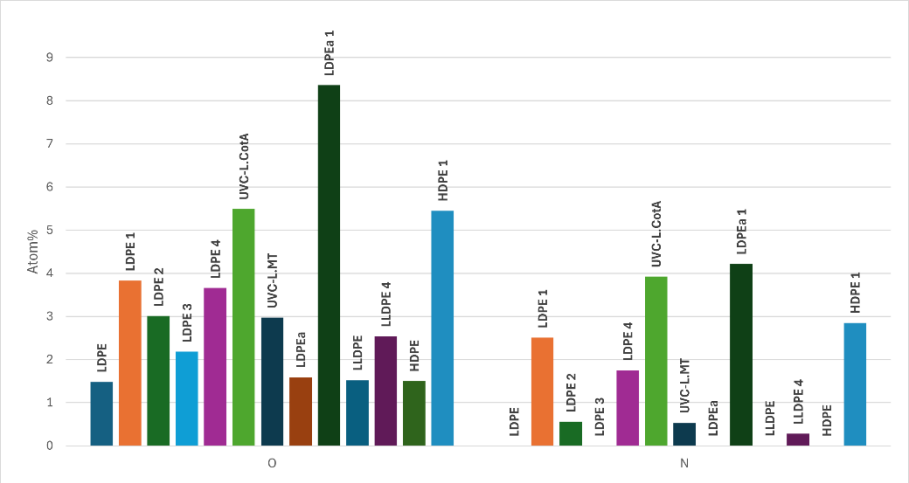

Figure 15: EDX results for PE films before and after chemoenzymatic treatment, showing the elemental composition of oxygen and nitrogen. LDPE, LDPEa, LLDPE and HDPE represents the untreated films. Sample IDs 1-4 correspond to the different chemical pretreatments followed by the enzymatic treatment: $KMnO_4$/HCl followed by L.CotA (1), Fenton followed by L.CotA (2), $KMnO_4$/HCl followed by L.MT (3) and Fenton followed by L.CotA (4). UVC-L.CotA and UVC-L.MT represents LDPE treated with UVC-Fenton followed by L.CotA and L.MT, respectively.

The thermal properties and calculated degree of crystallinity of the PE films before and after chemoenzymatic treatment are presented in Table 3. Among the untreated films, LLDPE exhibited the lowest melting temperature and degree of crystallinity, followed by LDPEa, while HDPE exhibited the highest values for both parameters. Following chemoenzymatic treatment, the thermal properties remained largely unchanged or slightly reduced. The only exception was LDPEa treated Fenton and L.CotA, for which the melting temperature had increased with 2 °C after treatment.

When comparing the DSC curves, see Appendix A10-12, most samples exhibited thermal behaviour similar to the untreated film. A noticeable exception was observed for LDPEa treated with Fenton followed by L.CotA, which displayed lower and broader melting and crystallisation peaks compared to the control.

Table 3: DSC data for LDPEa, LLDPE and HDPE films including melting temperature (T_m), melting enthalpy (ΔH_m) and calculated degree of crystallinity (X_c, %). The LDPEa, LLDPE and HDPE represent the untreated films. Sample IDs 1, 2 and 4 correspond to the different chemical pretreatments followed by the enzymatic treatment: $KMnO_4$/HCl followed by L.CotA (1), Fenton followed by L.CotA (2) and Fenton followed by L.CotA (4).

Sample	T_m (°C)	ΔH_m (J/g)	X_c (%)
LDPEa	**95.05**	**109.36**	**37.32**
1	94.11	106.17	36.24
2	97.28	95.73	32.67
LLDPE	**102.94**	**84.75**	**28.92**
2	102.71	81.69	27.88
4	102.92	83.49	28.49
HDPE	**119.17**	**213.34**	**72.81**
1	118.71	208.65	71.21

4.5 Identification of Degradation Products

HPLC analysis of the reaction mixture did not reveal any degradation products, see Appendix A13 for the chromatogram. However, GC-MS analysis of the reaction mixtures revealed peaks only present in the PE samples from 2 to 14 min, see Figure 16. The reaction mixtures from L.CotA treatments primarily exhibited peaks between 8 to 14 min, while those from L.MT treatments showed peaks between 2 to 12 min. Notably, Fenton combined with L.CotA resulted in significantly fewer peaks than L.CotA combined with $KMnO_4$/HCl. Overall, chemoenzymatic degradation using L.MT generated more peaks with greater intensities compared to L.CotA. The different PE films exhibited similar GC-MS peak patterns, although the reaction mixtures from LDPE treatment displayed significantly higher signal intensities, see Appendix A14.

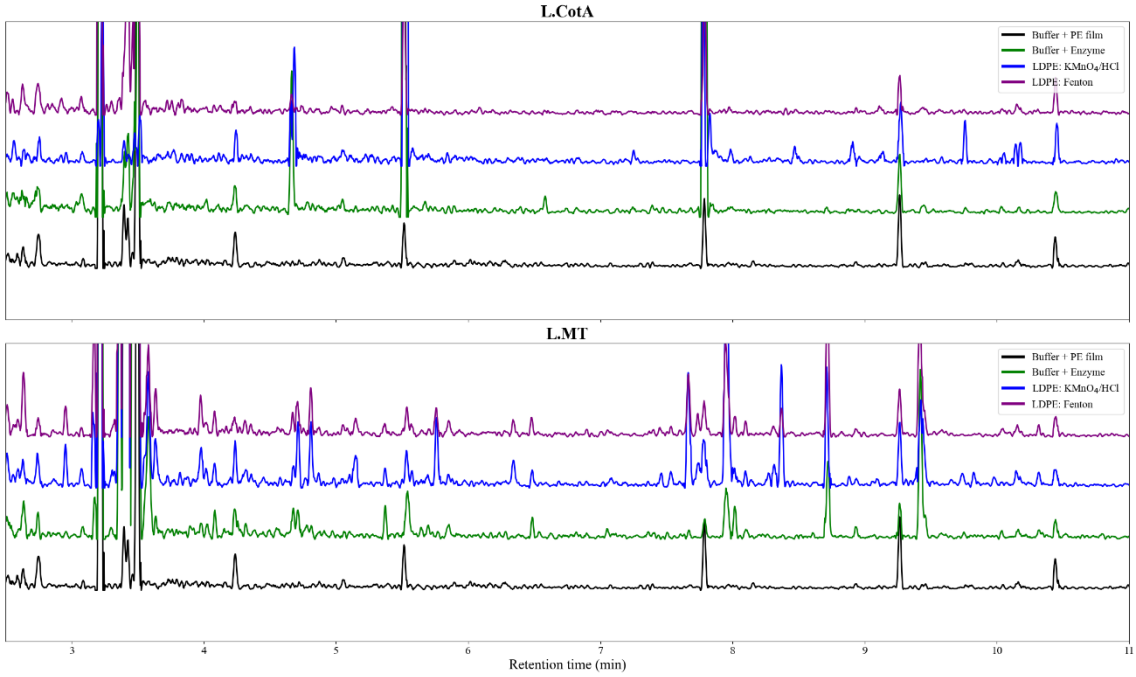

Figure 16: GC analysis of reaction mixture from LDPE treatment. The black curve represents a control sample containing buffer and pretreated film without enzyme. The green curve represents a control sample containing buffer and enzyme without film (L.CotA, top: L.MT, bottom). The blue curve represents films treated with $KMnO_4$/HCl followed by L.CotA (top) and L.MT (bottom). The purple curve represents films treated with Fenton oxidation followed by L.CotA (top) and L.MT (bottom).

The new peaks detected in Figure 16 were further identified with MS analysis using the NIST Mainlib database, retention time analysis and fragmentation pattern interpretation, the major compounds are presented in Table 4. Characteristic fragments for MSHFBA derivatisation are m/z 73 for trimethylsilyl (TMS), m/z 147 for di-TMS, m/z 117 for TMS-carboxylic acid, m/z 103 for primary TMS-alcohol and m/z 169 for heptafluorobutyric anhydride (HFB). (MACHEREY-NAGEL). The characteristic fragments for PE oligomers (m/z 43, 57, 71, 85, 99) were present in all peaks, therefore they are excluded from the table. Additionally, the m/z 77 fragment was present in reaction mixtures from LDPEa and is the characteristic fragment for a phenyl ion (NIST Chemistry WebBook, 2025).

The main degradation products were oxidised oligomers including hydroxy acids, dicarboxylic acids and fatty acids with carbon chain lengths ranging from C2 to C20. Based on the identified degradation products, the shorter oxidised compounds were predominantly found in reaction mixtures from L.MT treatment. Overall, treatment with L.MT resulted in a broader range of

degradation products. In addition, certain compounds, such as 14-hydroxytetradecanoic acid and 8-hydroxyoctanoic acid were exclusively found in reactions 1 and 3, both of which had $KMnO_4$/HCl as the chemical pretreatment. In contrast, treatment with L.CotA generally produced longer oxidised oligomers, with eicosanoic acid identified as the longest compound, found in reaction 2.

Table 4: Compounds identified by GC-MS analysis of reaction mixture following chemoenzymatic treatment. The listed compounds were detected as mixed MSHFBA derivatives and were exclusively detected in the samples and not the in the controls. Sample IDs 1-4 correspond to the different chemical pretreatments followed by the enzymatic treatment: $KMnO_4$/HCl followed by L.CotA (1), Fenton followed by L.CotA (2), $KMnO_4$/HCl followed by L.MT (3) and Fenton followed by L.CotA (4). The table includes the main fragments detected by MS and the base peaks are marked in bold.

RT (min)	Reaction ID	Main Fragments (m/z)	Compound (Detected as MSHFBA derivative)	Formula (Underivatised)	Compound Structure
2.16	3 4	**71**, 73, 117, 149, 169, 389	Glycolic acid	$C_2H_4O_3$	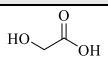
3.18	2 3 4	57, 100, **118**, 149, 169, 220	Lactic acid	$C_3H_6O_3$	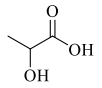
4.65	1 2 3	**73**, 117, 143, 169, 334, 382, 394	3-Hydroxybutanoic acid	$C_4H_8O_3$	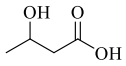
5.16	3 4	103, **131**, 169, 207, 323, 382, 394	5-Hydroxypentanoic acid	$C_5H_{10}O_3$	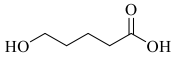
6.95	2 3 4	**42**, 73, 77, 131, 169, 191, 207 277, 333	6-Hydroxyhexanoic acid	$C_6H_{12}O_3$	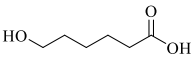
7.55	3 4	**73**, 103, 117, 131, 143, 147, 169, 396	2,3-Dihydroxyheptanedioic acid	$C_7H_{12}O_6$	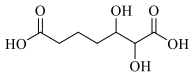
8.39	1 3	129, 143, 169, 199, **241**, 349, 384	8-Hydroxyoctanoic acid	$C_8H1_6O_3$	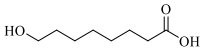
8.91	1 2 3	**73**, 77, 103, 135, 169, 171, 207, 336, 372	2-Hydroxynonanoic acid	$C_9H_{18}O_3$	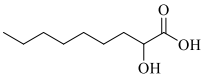
10.05	1 3	89, **103**, 116, 130, 143, 169, 207	14-Hydroxytetradecanoic acid	$C_{14}H_{28}O_3$	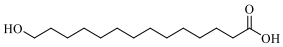
12.45	1 2 4	**57**, 133, 169, 191, 281, 382	Stearic acid	$C_{18}H_{36}O_2$	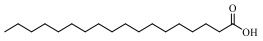
13.81	2	**55**, 77, 133, 169, 191, 281, 384, 391	Eicosanoic acid	$C_{20}H_{40}O_2$	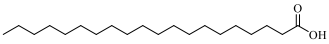

5. Discussion

5.1 Oxidative Modification of the Polymer Backbone

Two distinct chemical pretreatments, $KMnO_4$/HCl and Fenton oxidation, were investigated to increase the susceptibility of PE films to microbial attack and enhance the overall enzymatic efficiency. FTIR analysis of the PE films revealed distinct oxidation patterns following both chemical pretreatments. Treatment with $KMnO_4$/HCl resulted in a pronounced C=O peak at 1717 cm^{-1}. This aligns with previous studies, although those studies have also reported that the carbonyl peak is strongly influenced by the temperature, with higher temperatures promoting increased carbonyl formation (Fávaro, et al, 2007). In contrast, the results shown in Figure 7 indicate that increasing the operating temperature to 80°C only slightly increases the carbonyl peak**.** This suggests that the reaction is near its optimal temperature and has reached maximal oxidation. Therefore, the operating temperature was maintained at 60°C which is also more favourable from an energy and process sustainability perspective.

The optimised Fenton oxidation introduced new absorptions bands at 1110 cm^{-1}, 1540 cm^{-1}, 1715 cm^{-1} and 3370 cm^{-1} which corresponds to the formation of C-O, C=C, C=C and -OH groups. These results align with previous studies and suggest that the surface has been attacked by the hydroxyl radicals generated from the Fenton reaction (Ortiz, et al, 2022). After UVC treatment, a new absorption peak corresponding to a C-O bond appeared. This is consistent with previous studies reporting that UV treatment of PE primarily leads to the formation of C-O and O-H bonds. However, most of these studies utilised a significantly longer exposure time ranging from several hours to days (Ciuffi, Fratini, Emiliano, & Rosi, 2024). Therefore, the relatively weak C-O peak observed in this study is probably due to the short exposure time. When combining Fenton oxidation with UVC irradiation, the same peaks were formed but were more pronounced, which was further confirmed by the increase of the CI by a factor of 3. This is consistent with previous studies, the radical sites generated from the UVC irradiation were subsequently attacked during the Fenton oxidation (Lomwongsopon, et al, 2025).

Overall, these findings suggest that $KMnO_4$/HCl oxidation is more selective as it mainly promotes carbonyl formation whereas Fenton oxidation introduces a broader range of oxygenated functional groups to the polymer backbone, although with lower peak intensities. This is further evidenced by the CI, which is significantly higher for the treatment with $KMnO_4$/HCl compared to Fenton.

After chemoenzymatic treatment, both pretreatments successfully enhanced the oxidation of the PE films, as evidenced by the synergistic increase of the CI, compared to the separate treatments. This is in alignment with previous studies that have stated that a pretreatment step is necessary to enhance enzymatic degradation (Lomwongsopon, et al, 2025)**.** FTIR analysis after the chemoenzymatic treatment revealed the introduction of multiple oxygenated functional groups to the polymer backbone. In particular, the combination of $KMnO_4$/HCl oxidation with L.CotA treatment resulted in significant modifications, evidenced by pronounced C=O, C-O, O-H and C=C peaks.

Comparing FTIR spectra before and after enzymatic treatment revealed that the carbonyl peak at 1717 cm^{-1} formed during the chemical pretreatment step almost disappeared. In contrast, new absorption peaks corresponding to the C=O and C=C groups emerged at 1652 cm^{-1} and 1540 cm^{-1}, respectively. This trend is most evident in the L.CotA spectra and has been reported as evidence of polymer degradation in previous studies. It suggests that the PE backbone has undergone progressive oxidation and fragmentation rather than simple surface modification. In particular, the formation of C=C and OH groups can be interpreted as evidence of oxidation by hydroxylation, which is a crucial step in PE degradation (Zadeh, 2024).

In addition, enzymatic treatment followed by UVC-Fenton treatment increased the CI for L.CotA by a factor of 2.3 and for L.MT by a factor of 1.23 compared to Fenton alone. These results suggest that the choice of pretreatment directly influences the enzymatic efficiency, as well as what functional groups are introduced and to what degree. By integrating multiple treatments, the overall efficiency can be substantially increased. This is noteworthy, as one of the main limitations of the biotechnological recycling of plastics is its low efficiency, which explains the emerging trend in recent studies to use used mixed consortia of enzymes or microorganisms and apply multiple pretreatment steps.

Additionally, FTIR analysis of LDPE treated with UVC-Fenton suggests that when the pretreatment method is sufficiently effective, the laccase source has a lower impact on the overall efficiency. The oxidation patterns observed after UVC-Fenton pretreatment combined with both L.MT and L.CotA follow the previously described FTIR trends that suggest PE degradation. This behaviour was not observed to the same extent for L.MT when combined with the other pretreatments. This claim is further supported by the results obtained when L.MT is paired with $KMnO_4$/HCl, where the resulting CI for the combined treatments is lower than for the individual treatments. This effect was not observed for L.CotA and the difference may be because fungal laccases are generally more sensitive to their surrounding environment and more substrate specific, whereas bacterial laccases tend to be more robust.

Based on the FTIR analysis, L.MT is much more compatible with Fenton oxidation and L.CotA is slightly more compatible with $KMnO_4$/HCl oxidation. Overall, L.CotA is much more efficient in introducing oxygenated functional groups to the PE surface, as evidenced by the consistently higher CI for all films. Notably, one possible explanation is that the enzyme concentration and dosing strategy used to maintain catalytic activity were based on a protocol optimised for L.CotA. Therefore, it is possible that the fungal laccase would be more efficient under conditions optimised to its own activity profile.

All four films showed similar FTIR trends following both chemical and enzymatic treatment, but to different degrees. The highest CI was exhibited on LDPE, LDPEa and HDPE when combining $KMnO_4$/HCl with L.CotA while the CI for LLDPE was highest after Fenton combined with L.MT. Notably, LDPE and LDPEa generally exhibited a higher CI compared to LLDPE and HDPE. This trend aligns with the theory that polymers with a lower degree of crystallinity are more susceptible to degradation. This is because the first step in biological degradation, excluding pretreatment, involves enzyme adsorption to the polymer surface and a higher degree of crystallinity reduces the enzyme's accessibility to the PE bonds, resulting in limited bond cleavage and lower catalytic activity.

5.2 Morphological, Elemental & Thermal Modifications

As previously stated, the enzymatic oxidation process begins with enzyme adsorption to the polymer surface, leading to morphological, chemical and thermal modifications (Ortiz, et al, 2022). In this study, the observed morphological changes included fractures, surface roughening, crack formation, localised etching and the accumulation of white clusters of particles. Notably, surface defects were also observed in the untreated films, these are likely from a combination of extrusion during manufacturing and sample preparations prior to SEM analysis. These defects were most extreme for the LLDPE films.

EDX analysis of untreated films exhibited an oxygen content of around 1.5 atom%. This is most likely due to instrumental limitations in detecting lighter elements and the inability to measure hydrogen. Therefore, 1.5 atom% served as the baseline for all other measurements. Following chemoenzymatic treatment, the oxygen content increased in all samples and the elemental mapping

revealed a uniform distribution of oxygen across the surface, confirming successful and homogenous oxidation of the polymer.

In general, samples with higher oxygen content also had increased nitrogen content which was absent in the untreated PE films. The presence of nitrogen is attributed to the laccase enzyme, suggesting successful adsorption of the enzyme to the surface. Additionally, the more pronounced morphological changes observed in the SEM images were consistent with the increased oxygen content detected by EDX, supporting the claim that extensive surface oxidation had occurred.

Interestingly, LDPEa exhibited the highest oxygen and nitrogen content overall, indicating that the antioxidants originally present may have been partially released or consumed during the pretreatment and enzyme treatment. This, in turn, may have increased the susceptibility to chemoenzymatic modification and contributed to the observed morphological and elemental modifications. This interpretation is further supported by the detection of a m/z 77 fragment corresponding to a phenyl ion. In previous studies, the presence of antioxidants or additives in the released products has been used as indirect proof of PE degradation (Yao, et al, 2022).

Furthermore, DSC analysis of the untreated films revealed that HDPE had the highest crystallinity and melting temperature, followed by LLDPE and LDPEa. This trend is consistent with the theoretical expectations presented in the background sections. The thermal behaviour remained very similar before and after pretreatment with a slight decrease in both melting temperature and crystallinity for all PE films. One exception was observed for LDPEa treated with Fenton followed by L.CotA, in this case, the melting temperature had increased slightly and more pronounced changes were observed in the DSC curves, including the reduction and broadening of the melting and crystallisation peaks. These observations suggest that treatment with L.CotA resulted in thermal modifications of LDPEa. These trends are consistent with previous studies on polymer biodegradation, where crystallinity decreased from 63% to 52% following a 140 day treatment. Crystallinity is considered one of the main factors that limit the efficiency of the biodegradation of polyolefins, as a higher degree of crystallinity reduces the accessibility to enzymes and oxidative species (Lee, et al, 2023).

Taken together, the observed morphological changes, together with the increased oxygen content and slightly reduced thermal properties confirm that the enzymes have successfully induced oxidation and structural modifications in the polymers. Furthermore, these results indicate that the presence of antioxidants impacts the morphological, elemental and thermal modifications in ways that are not observed for the other films, whose oxidation trends closely align with theoretical expectations and previous studies.

5.3 Degradation products & Potential Applications

The identification of oxidative degradation products ranging from C2 to C20 is further evidence of the chemoenzymatic modification of the PE backbone. The enzymes have not only adsorbed to the surface, but depolymerisation into smaller fragments has also started. The release of dicarboxylic and hydroxy acids is consistent with the oxygenated functional groups observed with FTIR and the increased oxygen content detected with EDX, further supporting the claim of oxidative modification of PE.

The identified degradation products are consistent with the proposed degradation mechanism. First, the laccase-mediator system cleaves the C-H bonds of the PE backbone, after which progressive oxidation and the incorporation of oxygenated functional groups lead to further chain scission, ultimately yielding small oxidative products (Ding, et al, 2026). This pathway is directly reflected in the identified compounds, where longer oxidised chains, such as eicosanoic acid, represent the

first stage, followed by the formation of more extensively oxidised intermediates, such as 2,3-dihydroxyheptanedioic acid. Which are eventually broken down into small, oxidised compounds, such as glycolic acid. The presence of these compounds suggests a stepwise degradation following the chemoenzymatic process.

Treatment with L.CotA primarily generated longer oxidised oligomers, indicating that degradation was largely surface limited. In contrast, treatment with L.MT produced a broader product range, including short-chain hydroxy acids and highly oxidised intermediates, suggesting more extensive degradation of the polymers. Furthermore, combining L.CotA with $KMnO_4$/HCl resulted in significantly more intense peaks than when it was combined with Fenton. For L.MT, there was no observable trend for the pretreatments, despite previous results in this study has shown that it is less compatible with $KMnO_4$/HCl. These results are consistent with a previous study that reported distinct degradation patterns for bacterial and fungal laccases. Bacterial laccases predominantly generated oxidised degradation products with a chain length of C7 to C15, whereas fungal laccases produced shorter oxidised products with a chain length of C4 to C8. Additionally, the fungal laccase generated a greater diversity of oxidation products, including esters, carboxylic acids, ketones and alcohols, compared to the bacterial laccase (Yao, et al, 2022).

Taken together with the high CI, the morphological and elemental modifications with the larger amount and more intense peaks observed in the GC-MS analysis it can be stated that LDPE is easier to modify through chemoenzymatic treatments compared to the other films, although the difference is not major. Overall, the differences in degradation and modification behaviour among the films are in agreement with the theoretical expectation that enzymes are substrate specific and that their catalytic efficiency is affected by the substrate properties. This substrate dependency is one of the key challenges for the development of efficient biotechnological recycling.

In this study, the identified degradation products were exclusively carboxylic acids with varying chain lengths. This finding is consistent with the study on PE degradation using mCPBA and ultrasonication followed by treatment with a multi-enzyme complex. In that study, the identified products where 7-hydroxyheptanoic acid, 9-hydroxynonanoic acid, 11-hydroxyundecanoic acid, 14-hydroxytetradecanoic acid, 16-hydroxyhexadecanoic acid, sebacic acid, undecanedioic acid, dodecanedioic acid and tridecanedioic acid (Oiffer, et al, 2024).

In addition, a study on the chemoenzymatic degradation of HDPE reported carboxylic acids and alkanes as the degradation products. The identified carboxylic acids were decanoic acid, docosanoic acid, undecanoic acid, deconoic acid, hexadeconoic acid, propanoic acid, oleic acid, oxalic acid, cyclopropanetetradecanoic acid, benzene dicarboxylic acid, phthylic acid, octadecatrienoic acid, acetic acid, hexanoic acid, octadecanoic acid, butanoic acid, oxaminmidic acid, undecanoic acid, docosanoic acid, tetradecanoic acid and propyldodecanoic acid (Balasubramanian, et al, 2014).

From a recyclability perspective, it is beneficial to evaluate the potential applications and upcycling opportunities of the generated degradation products, as this represents a key advantage of biotechnological recycling compared to conventional recycling methods.

The ultrashort hydroxy acids can be used as building blocks for the synthesis of biodegradable polymers and copolymers. For example, glycolic acid is used in the production of polyglycolic acid (PLGA) while lactic acid is used to synthesise polylactic acid (PLA). PLGA is especially known for its biodegradability and biocompatibility, making it particularly suitable for medical and therapeutic applications. Lactic acid can also be used as a food preservative and moisturising agent in cosmetic applications. In fact, the cosmetic field represents one of the major areas of use for these compounds due to their antibacterial and anti-inflammatory properties. These characteristics, combined with their demonstrated antitumor effects also make them attractive for pharmaceutical applications (Bhalla, et al, 2014).

Another interesting class of compounds is the polyoxidised hydroxy acids, which can be used as key intermediates in biobased and green chemistry to produce sustainable products and materials, such as biodegradable polymers (Jiemeng, 2019). These biodegradable plastics have been shown to generate lower carbon dioxide emissions than conventional fossil-based plastics, thereby contributing less to global warming. As a result, they are considered a promising sustainable alternative to petroleum-derived plastics. With the growing focus on environmental sustainability and green chemistry, biobased and biodegradable compounds have attracted considerable attention from both industry and academia, as reflected by the extensive research in this field (Bhalla, et al, 2014).

Furthermore, the identification of unsaturated fatty acids is of considerable industrial interest, as these compounds can serve as building blocks for a wide range of everyday products. The applications of fatty acids largely depend on their carbon chain length and degree of saturation. Short to medium chain fatty acids are particularly suitable for solvent and cleaning applications, such as detergents. From an industrial perspective, fatty acids in the C8 to C22 range are the most relevant, as longer chains give the material higher thermal stability, making them more attractive for more demanding applications. These compounds are used in products such as lubricants, fuel additives, waxes, personal care products, advanced paints, coatings and adhesives (Hanson Chemicals, 2026)

Overall, L.MT appears to be the better choice solely from a recyclability perspective, as it produces a broader range of degradation products with great potential for industrial application and upcycling. Still, both bacterial and fungal laccases demonstrate significant potential in PE degradation, with overall efficiency likely to be improved trough the optimisation of the oxidation and enzymatic steps as well as enhanced compatibility with the plastic waste. However, the absence of detectable products from HPLC, the relatively low intensity of the GC-MS peaks, the limited surface modifications and most importantly, the minor changes in thermal properties collectively indicate that the current chemoenzymatic treatment predominantly results in surface-level modifications, potentially suggesting early signs of polymer degradation.

6. Conclusion & Future Work

In conclusion, the chemoenzymatic treatment successfully modified the polyolefin films through surface oxidation, indicating early stages of polymer degradation. Combining chemical pretreatments with enzymatic degradation enhanced the oxidation of the polymer backbone. The choice of pretreatment directly influenced the overall efficiency and compatibility of the enzymes. L.CotA was more compatible with $KMnO_4$/HCl, primarily generating longer oxidised oligomers indicating more surface limited modification. In contrast, L.MT was more effective paired with Fenton oxidation generating a broader range of degradation products suggesting more extensive degradation. By integrating UVC irradiation with Fenton oxidation, the chemical and enzymatic efficiency was improved. Thermal and morphological modifications were confirmed by the presence of surface cracks, particle clusters, increase in oxygen content and a slight decrease in melting temperature and crystallinity. LDPE and LDPEa proved to be most susceptible to chemoenzymatic modification. Finally, the identified degradation products ranging from ultra short hydroxy acids to longer fatty acids have significant potential for upcycling into biodegradable polymers as well as for applications across a range of industrial sectors.

For future work, the polymers should be analysed with HT-GPC and surface contact angle to investigate changes in molecular weight and hydrophobicity following chemoenzymatic treatment. To make the study more accurate, UVC-Fenton should be performed on all LDPEa, LLDPE and HDPE as well and the enzymatic activity of the commercial L.MT should be quantified and the enzyme dosages should be adjusted accordingly to ensure that L.CotA and L.MT are compared at equivalent activity. To further optimise the pretreatment step, future work could investigate the combination of UVC irradiation with $KMnO_4$/HCl as well as investigate UVC-H_2O_2 treatment as a a greener approach. For the enzymatic treatment, future studies could investigate the effects of combining L.MT and L.CotA on PE oxidation. This strategy would be interesting because enzymes mixtures have shown promising effects in recent studies. In addition to this, future studies could investigate the effects of extended reaction times or elevated temperatures. Finally, while this study included LDPEa to investigate how the chemoenzymatic treatment performed in the presence of additives, it would be interesting to use real mixed post-consumer plastic waste in future work.

Acknowledgement

I would like to thank my supervisors Sang Hyun Pyo, Mohamed Ismail and Åsa Olsson for their support and guidance throughout this thesis work. I would also like to thank Rajni Hatti-Kaul for being the examiner for this master thesis. Thank you to Daniel Madsen for assistance with SEM and EDX analysis, Lars Dahlgren support with GC-MS analysis and Cecilia Håkansson for helping me with the DSC measurements. I would like to thank the entire Department of Biotechnology for the assistance and support with laboratory work and instruments, especially with all the help and guidance regarding the enzymes. Thank you Tetra Pak for making this thesis possible and for the opportunity to collaborate. Finally, I would like to express my appreciation for the learning experience this project has provided, I have learnt a lot and truly enjoyed the work.

References

Andrea, C., Enrico, M., Antonella, M., Gabriele, P., Filippo, P., Pier, F. M., Valter, C. (2024). *Natural iron-containing minerals catalyze the degradation of polypropylene microplastics: a route to self-remediation learnt from the environment.* Retrieved from https://doi.org/10.1007/s11356-024-34120-0

Balasubramanian, V., Natarajan, K., & Rajeshkannan, V. (2014). *Enhancement of in vitro high-density polyethylene (HDPE) degradation by physical, chemical, and biological treatments.* Retrieved from https://doi.org/10.1007/s11356-014-3191-2

Bhalla, T. C., Kumar, V., & Bhatia S. K (2014). *Hydroxy Acids: Production and Applications.* Retrieved from https://www.researchgate.net/publication/311494113_Hydroxy_Acids_Production_and_Applications

Charitopoulou, M.-A., & Achilias, D. S. (2026). *Identification and Recycling of Polyolefins: Case Study of PE and PP.* Retrieved from https://doi.org/10.1021/acs.iecr.5c03923

Ciuffi, B., Fratini, Emiliano, & Rosi, L. (2024). *Plastic pretreatment: The key for efficient enzymatic and biodegradation processes.* Retrieved from https://doi.org/10.1016/j.polymdegradstab.2024.110698

Cremerna. (2021). *Fatty Acids and Industrial Products*. Retrieved from https://www.petercremerna.com/fatty-acids-and-industrial-products/

Ding, R., Xu, L., Shan, X., Qiu, X., Ding, L., Zhang, B., . . . Guo, X. (2026). *Enhanced degradation of microplastics by laccase under ambient conditions: Analysis of underlying molecular mechanisms.* Retrieved from https://doi.org/10.1016/j.jhazmat.2026.141109

Dokl, M., Copot, A., & Krajnc, D. (2024). *Global projections of plastic use, end-of-life fate and potential changes in consumption, reduction, recycling and replacement with bioplastics to 2050.* Retrieved from https://doi.org/10.1016/j.spc.2024.09.025

Entzimatiko. (2026). Retrieved from Entzimatiko : https://entzimatiko.com/

Fávaro, S., Rubira, A., Muniz, E., & Radovanovic, E. (2007). *Surface modification of HDPE, PP, and PET films with KMnO4/HCl solutions.* Retrieved from https://doi.org/10.1016/j.polymdegradstab.2007.04.005

Fentons Reagent General Chemistry Using H2O2. (u.d.). USP technologies solutions for a clean environment. Retrieved from https://usptechnologies.com/fentons-reagent-general-chemistry-using-h2o2/

García, L., Florindo, R., Saez, V., Wojcieszak, R., Ramon, J., & Itabaiana Jr. (2024). *Enhanced Thermostability of Laccase from Myceliophthora thermophila Through Conjugation with mPEG-SC.* Retrieved from https://doi.org/10.3390/catal14120887

Hadigheh, S., Wei, Y., Fernandes, K., Tao, Y., Bajan, S., & Carter, D. (2025). *Surface-level microbial-assisted biodegradation of polyolefin thermoplastics for enhanced energy efficiency and emission reduction.* Retrieved from https://doi.org/10.1016/j.susmat.2025.e01762

Hae Jin, J., Joon-Yung, C., Jung Hoon, C., Kyoung-Soon, J., Jongkoo, L., Woe-Yeon, K., . . . Jong-Rok, J. (2018). *One-Pot Transformation of Technical Lignins into Humic-Like Plant Stimulants through Fenton-Based Advanced Oxidation: Accelerating Natural Fungus-Driven Humification.* Retrieved from https://pubs.acs.org/doi/10.1021/acsomega.8b00697

Hanson Chemicals. (2026). *Understanding Fatty Acid Profiles and Their Role in High-Performance Formulations*. Retrieved from https://hansonchemicals.com/fatty-acid-profiles-and-their-role/

Hou, Y., Zhao, L., Yue, C., Yang, J., Zheng, Y., Peng, W., & Lei, L. (2024). *Enhancing catalytic efficiency of Bacillus subtilis laccase BsCotA through active site pocket design.* Retrieved from https://doi.org/10.1007/s00253-024-13291-3

Jeong, H. J., Cha, J.-Y., Choi, J. H., Jang, K.-S., Lim, J., Kim, W.-Y., . . . Jeon, J.-R. (2018). *One-Pot Transformation of Technical Lignins into Humic-Like Plant Stimulants through Fenton-Based Advanced Oxidation: Accelerating Natural Fungus-Driven Humification.* Retrieved from https://doi.org/10.1021/acsomega.8b00697

Jiemeng, L. (2019). *Biobased chemistry and technology: derivatives of aldaric acid as key intermediates for sustainable products and materials.* Retrieved from https://www.politesi.polimi.it/handle/10589/144247

Kong, D., Wang, L., Yuan, Y., Xia, W., Liu, Z., Shi, M., & Wu, J. (2024). *Review of key issues and potential strategies in bio-degradation of polyolefins.* Retrieved from https://doi.org/10.1016/j.biortech.2024.131557

Lee, G. H., Kim, D.-W., Jin, Y. H., Kim, S. M., Lim, E. S., Cha, M. J., . . . Ahn, J. H. (2023). *Biotechnological Plastic Degradation and Valorization Using Systems Metabolic Engineering.* Retrieved from https://doi.org/10.3390/ijms242015181

Li, X., Tian, J., Ren, X., Wang, J., & Liu, X. (2025). *Enhancement in the Catalytic Properties of CotA Laccase from Bacillus pumilus via High-Throughput Screening Using Malachite Green as a Pressure.* Retrieved from https://doi.org/10.3390/microorganisms13020377

Lomwongsopon, P., Martínez, B. M., Jiménez, A. B., Bardenstein, A. L., Kusano, Y., Christiansen, J. d., & Varrone, C. (2025). *Enhancing biodegradation of polyolefins and real mixed plastic waste by combination of pretreatment and mixed microbial consortia.* Retrieved from https://doi.org/10.1016/j.chemosphere.2025.144151

MACHEREY-NAGEL. (u.d.). *Derivatization reagents for GC.* Retrieved from https://www.mn-net.com/media/pdf/3c/d7/65/instructions-brochure-gc-derivatization-reagents.pdf

More, S. S., S, P., Renuka, K. P., M, S., Malini, S., & S M, V. (2011). *Isolation, Purification, and Characterization of Fungal Laccase from Pleurotus sp.* Retrieved from 10.4061/2011/248735.

NETZSCH. (2026). Retrieved from https://analyzing-testing.netzsch.com/en/polymers-netzsch-com/commodity-thermoplastics/pe-hd-polyethylene-high-density

NIST Chemistry WebBook. (2025). Retrieved from https://webbook.nist.gov/chemistry/

Oiffer, T., Friedemann, L., Süss, P., Breite, D., Griebel, J., & Khurram, M. (2024). *Chemo-Enzymatic Depolymerization of Functionalized Low-Molecular-Weight Polyethylene* . Retrieved from https://doi.org/10.1002/ange.202415012

Ortiz, D., Munoz, M., Nieto-Sandoval, J., Romera-Castillo, C., M. de Pedro, Z., & A. Casas, J. (2022). *Insights into the degradation of microplastics by Fenton oxidation: From surface modification to mineralisation.* Retrieved from https://doi.org/10.1016/j.chemosphere.2022.136809

Panwar, V., Lzaod, S., & Dutta, T. (2023). *Thermostable Bacterial Laccase: Catalytic Properties and Its Application in Biotransformation of Emerging Pollutants.* Retrieved from https://doi.org/10.1021/acsomega.3c03627

Shaoqin, C., & Yun Hang, H. (2024). *Complete Degradation of Polyolefin Plastic Wastes to HighValue Products.* Retrieved from doi.org/10.1002/cssc.202301449

Shuaibing, W., Hong, Y., Wei, L., Enze, S., Zhiguo, Z., Jing, X., . . . Zhihong, X. (2024). *Biodegradation of four polyolefin plastics in superworms (Larvae of Zophobas atratus) and effects on the gut microbiome.* Retrieved from https://doi.org/10.1016/j.jhazmat.2024.135381

Soong, Y.-H. V., Sobkowicz, M. J., & Xie, D. (2022). *Recent Advances in Biological Recycling of Polyethylene Terephthalate (PET) Plastic Wastes.* Retrieved from https://doi.org/10.3390/bioengineering9030098

Temporiti, M. E., Nicola, L., Nielsen, E., & Tosi, S. (2022). *Fungal Enzymes Involved in Plastics Biodegradation.* Retrieved from 10.3390/microorganisms10061180

Van Belle, A., Demets, R., Mys, N., Van Kets, K., Dewulf, J., Van Geem, K., Ragaert, K. (2020). *Microstructural Contributions of Different Polyolefins to the Deformation Mechanisms of Their Binary Blends.* Retrieved from doi: 10.3390/polym12051171

Xiaoyu, S., Ziyi, X., Zhihua, C., Junliang, W., Zhiyan, P., Zhong-Ting, H., & Mian, H. (2026). *Polyolefins pyrolysis: quantitative structure-thermal-reactivity relationships for selective high-value fuels and chemicals production.* Retrieved from https://doi-org.ludwig.lub.lu.se/10.1016/j.cej.2025.171974

Yao, C., Xia, W., Dou, M., Du, Y., & Wu, J. (2022). *Oxidative degradation of UV-irradiated polyethylene by laccase-mediator system.* Retrieved from https://doi.org/10.1016/j.jhazmat.2022.129709

Yingnan, S., Ge, B., Bian, X., Li, L., Fu, W., Wang, J., & Wang, Y. C. (2026). *Degradation Behavior of Original and Recycled Thermoplastic Polyolefin (TPO) After Ultraviolet (UV) Ageing.* Retrieved from https://link.springer.com/article/10.1007/s11665-026-13154-0

Yizhi, L., Donghuan, S., Yilin, Z., Xianrui, L., Yiming, Z., Gang, X., . . . Haijia, S. (2025). *Insights into polyolefin oligomer stress regulation of microbial communities and degradation mechanisms of polyethylene.* Retrieved from https://doi.org/10.1016/j.jenvman.2025.127969

Younus, H., Khan, M. A., Khan, A., & Alhumaydhi, F. A. (2025). *Eco-Friendly Biocatalysts: Laccase Applications, Innovations, and Future Directions in Environmental Remediation.* Retrieved from https://doi.org/10.3390/catal15100921

Yuxing, Z., D. Y., Xu, L., Peng-An, C., Xiukuan, Y., & Zhongbao, J. (2025). *Advances in sustainable polyolefins: synthesis, chemical transformation and recycling.* Retrieved from https://doi.org/10.1093/nsr/nwaf489

Zadeh, M. H. (2024). *Chemoenzymatic Oxidation of polyolefins* .

Zampolli, J., Mangiagalli, M., Vezzini, D., Lasagni, M., Ami, D., Natalello, A., . . . Di Gennaro, P. (2023). *Oxidative degradation of polyethylene by two novel laccase-like multicopper oxidases from Rhodococcus opacus R7.* Retrieved from https://doi.org/10.1016/j.eti.2023.103273

Zandieh, M., Griffiths, E., Waldie, A., Li, S., Honek, J., Rezanezhad, F., . . . Liu, J. (2023). *Catalytic and biocatalytic degradation of microplastics.* Retrieved from https://doi.org/10.1002/EXP.20230018

Zhang, N., Ding, M., & Yuan, Y. (2022). *Current Advances in Biodegradation of Polyolefins.* Retrieved from https://doi.org/10.3390/microorganisms10081537

Zhang, Y., Yang, D., Li, X., Chen, P.-A., Yao, X., & Jian, Z. (2025). *Advances in sustainable polyolefins: synthesis, chemical transformation and recycling.* Retrieved from https://doi.org/10.1093/nsr/nwaf489

Appendix

FTIR results

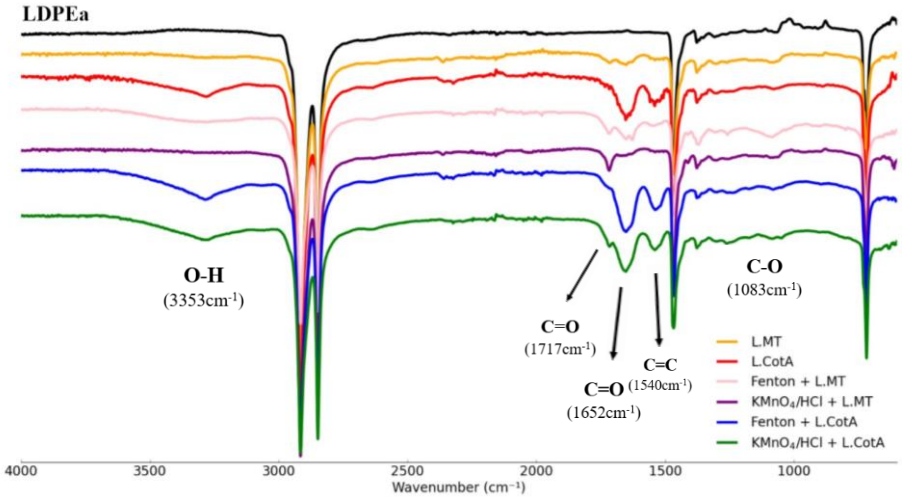

Figure A1: FTIR spectra of LDPEa films following chemoenzymatic treatment. The black curve corresponds to the untreaded film, while the orange (L.MT) and red (L.CotA) curves correspond to films after enzymatic treatment alone. The pink and purple curves correspond to films pretreated with Fenton oxidation and $KMnO_4$/HCl oxidation, respectively, followed by treatment with L.MT. The blue and green curves correspond to films pretreated with Fenton oxidation and $KMnO_4$/HCl oxidation, respectively, followed by treatment with L.CotA

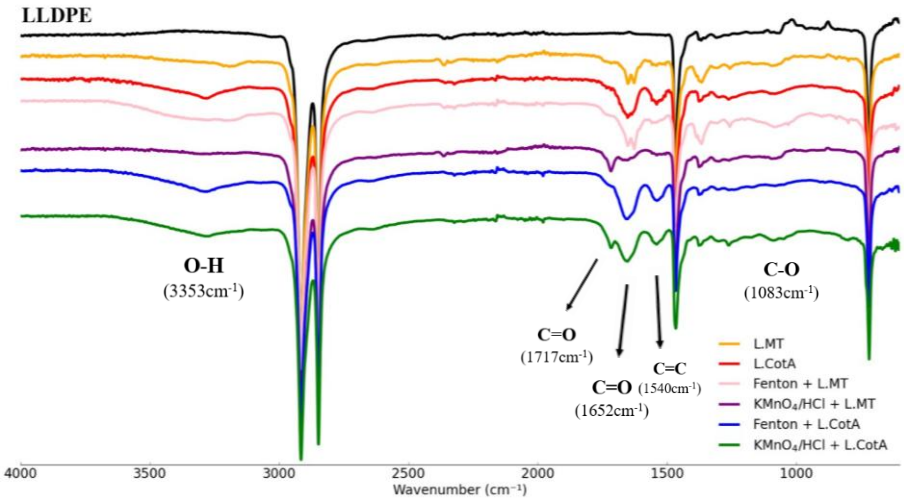

Figure A2: FTIR spectra of LLDPE films following chemoenzymatic treatment. The black curve corresponds to the untreaded film, while the orange (L.MT) and red (L.CotA) curves correspond to films after enzymatic treatment alone. The pink and purple curves correspond to films pretreated with Fenton oxidation and $KMnO_4$/HCl oxidation, respectively, followed by treatment with L.MT. The blue and green curves correspond to films pretreated with Fenton oxidation and $KMnO_4$/HCl oxidation, respectively, followed by treatment with L.CotA

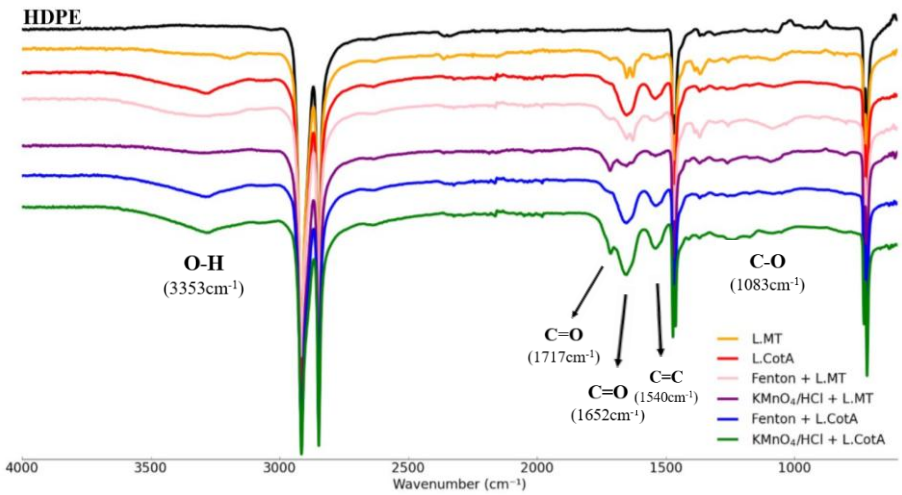

Figure A3: FTIR spectra of HDPE films following chemoenzymatic treatment. The black curve corresponds to the untreaded film, while the orange (L.MT) and red (L.CotA) curves correspond to films after enzymatic treatment alone. The pink and purple curves correspond to films pretreated with Fenton oxidation and $KMnO_4$/HCl oxidation, respectively, followed by treatment with L.MT. The blue and green curves correspond to films pretreated with Fenton oxidation and $KMnO_4$/HCl oxidation, respectively, followed by treatment with L.CotA

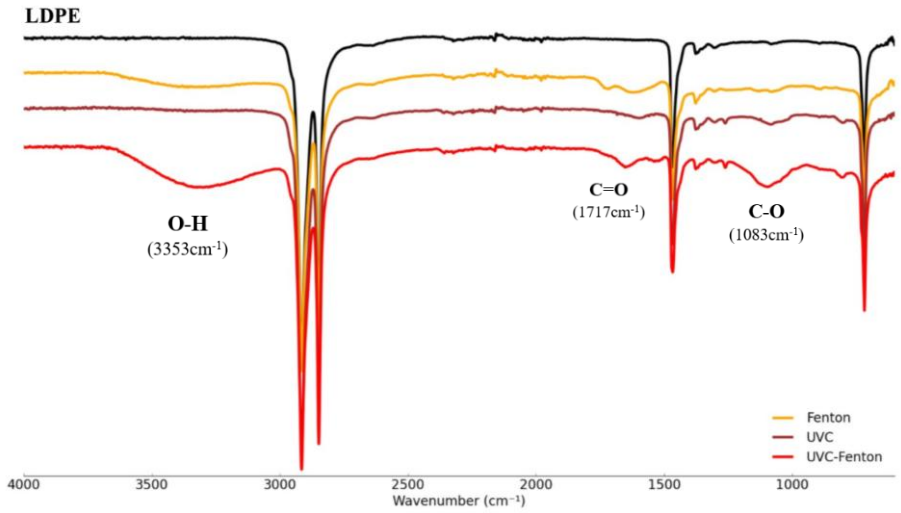

Figure A4: FTIR spectra of LDPE films before and after Fenton oxidation, UVC treatment and combined UVC-Fenton treatment. The black curve represents the untreated film, the orange curve represents the film after Fenton oxidation, the brown curve represents the film after UVC treatment and the red curve represents the film after Fenton oxidation of the UVC treated film.

SEM results

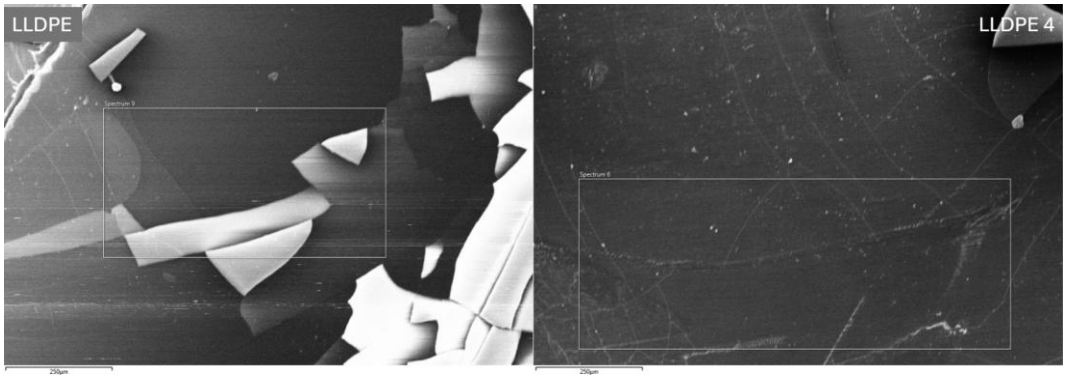

Figure A5: SEM images of untreated LLDPE (left) and LLDPE treated with Fenton followed by L.MT (LLDPE 4, right). The white boxes are the selected regions for EDX analysis, both images are taken at x100 magnification.

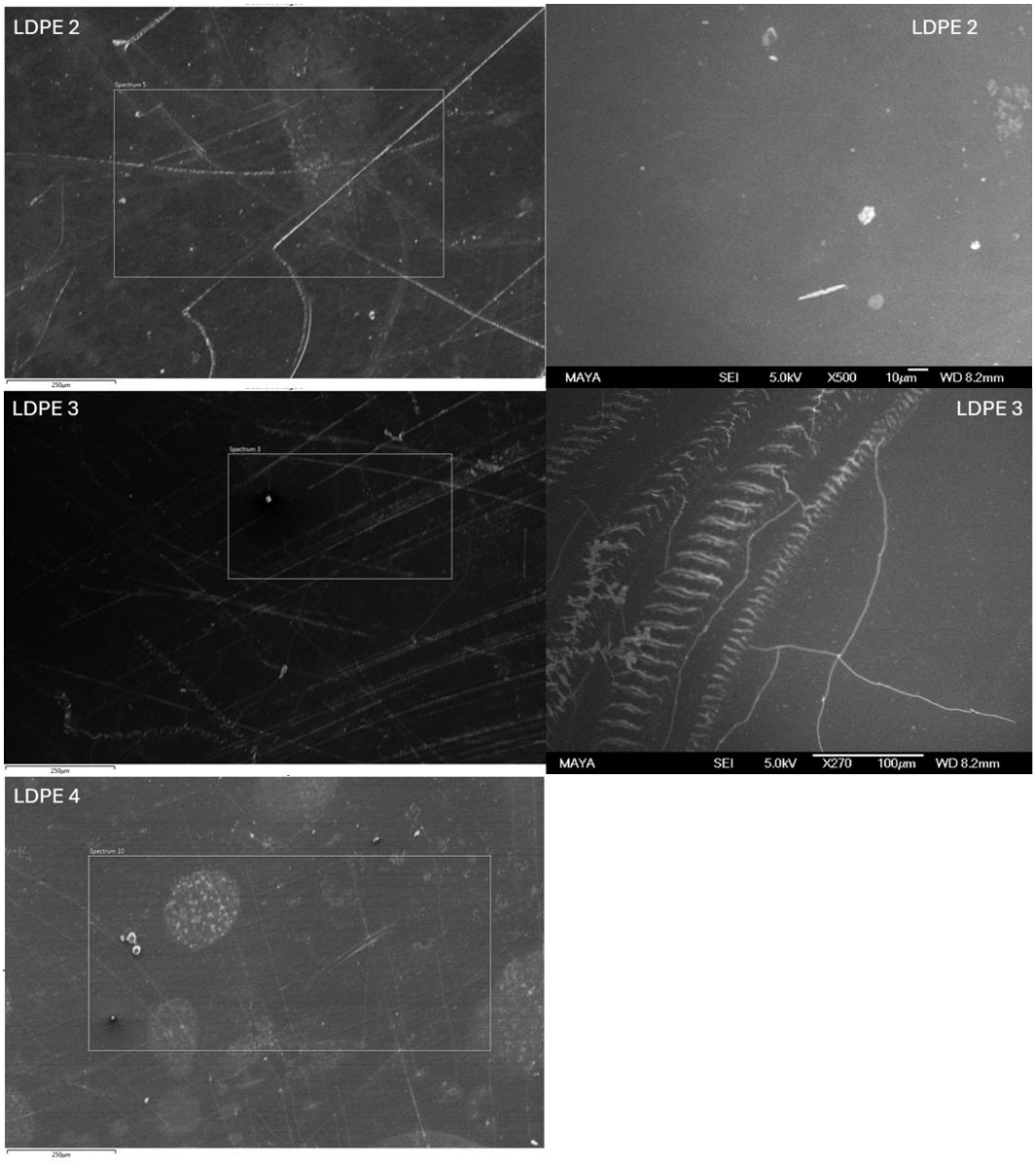

Figure A6: SEM images of LDPE films treated with Fenton followed by L.CotA (top), $KMnO_4$/HCl followed by L.MT (middle) and Fenton followed by L.MT (bottom). The white boxes are the selected regions for EDX analysis.

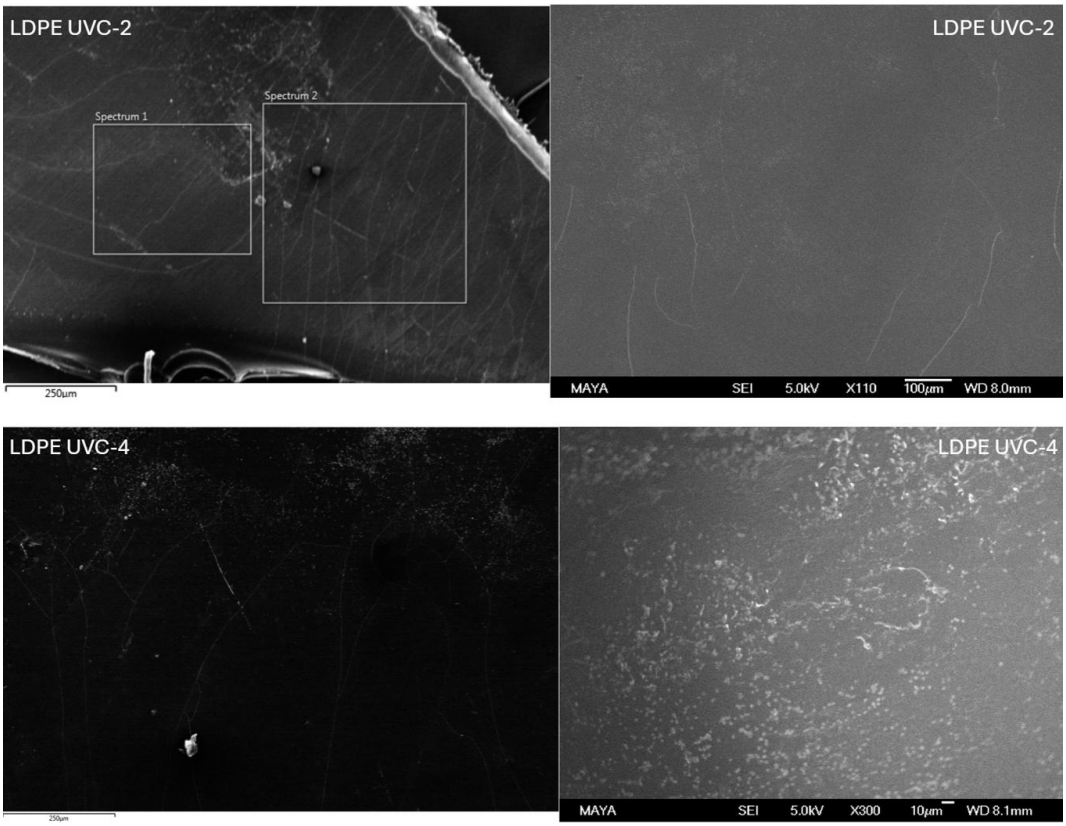

Figure A7: SEM images of LDPE films treated with UVC-Fenton followed by enzymatic treatment with L.CotA (top) and L.MT (bottom). The white boxes are the selected regions for EDX analysis.

EDX results

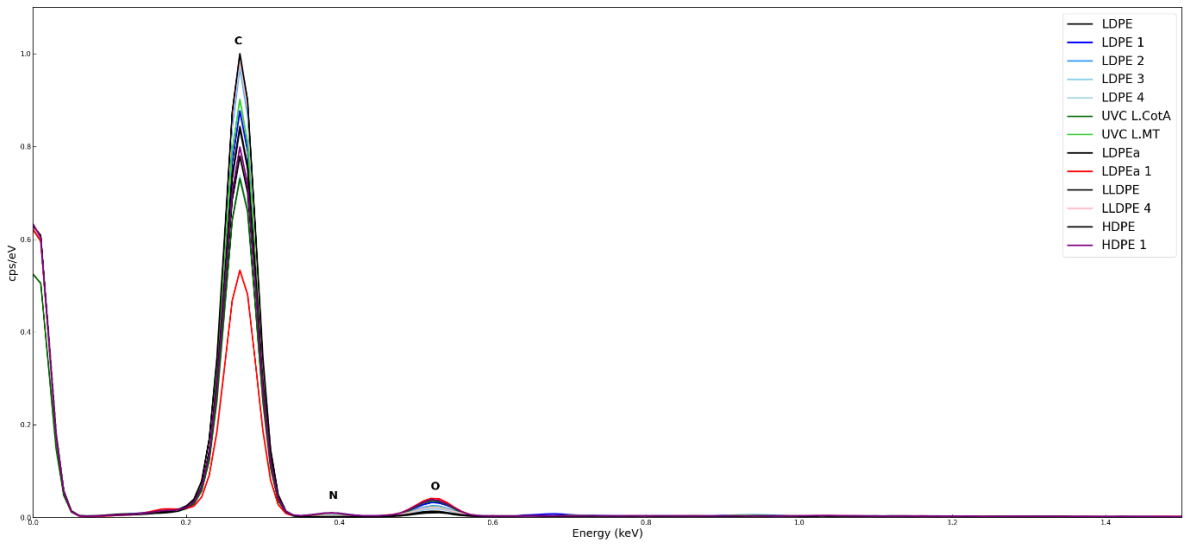

Figure A8: EDX spectra Overlay of all 13 samples. LDPE, LDPEa, LLDPE and HDPE represents the untreated films. Sample IDs 1-4 correspond to the different chemical pretreatments followed by the enzymatic treatment: $KMnO_4$/HCl followed by L.CotA (1), Fenton followed by L.CotA (2), $KMnO_4$/HCl followed by L.MT (3) and Fenton followed by L.CotA (4). UVC-L.CotA and UVC-L.MT represents LDPE treated with UVC-Fenton followed by L.CotA and L.MT, respectively.

Table A9: Elemental compositions of carbon, nitrogen and oxygen, detected with EDX. LDPE, LDPEa, LLDPE and HDPE represents the untreated films. Sample IDs 1-4 correspond to the different chemical pretreatments followed by the enzymatic treatment: $KMnO_4$/HCl followed by L.CotA (1), Fenton followed by L.CotA (2), $KMnO_4$/HCl followed by L.MT (3) and Fenton followed by L.CotA (4). UVC-L.CotA and UVC-L.MT represents LDPE treated with UVC-Fenton followed by L.CotA and L.MT, respectively.

Sample	C (Atom%)	N (Atom%)	O (Atom%)
LDPE	**98.52**	**n.d**	**1.48**
1	92.31	2.51	3.83
2	96.38	0.56	3.01
3	97.80	n.d	2.18
4	94.56	1.75	3.66
UVC-2	90.59	3.92	5.49
UVC-4	96.49	0.53	2.97
LDPEa	**98.40**	**n.d**	**1.59**
1	87.37	4.22	8.36
LLDPE	**98.45**	**n.d**	**1.52**
4	97.13	0.28	2.54
HDPE	**98.49**	**n.d**	**1.50**
1	91.67	2.85	5.45

DSC results

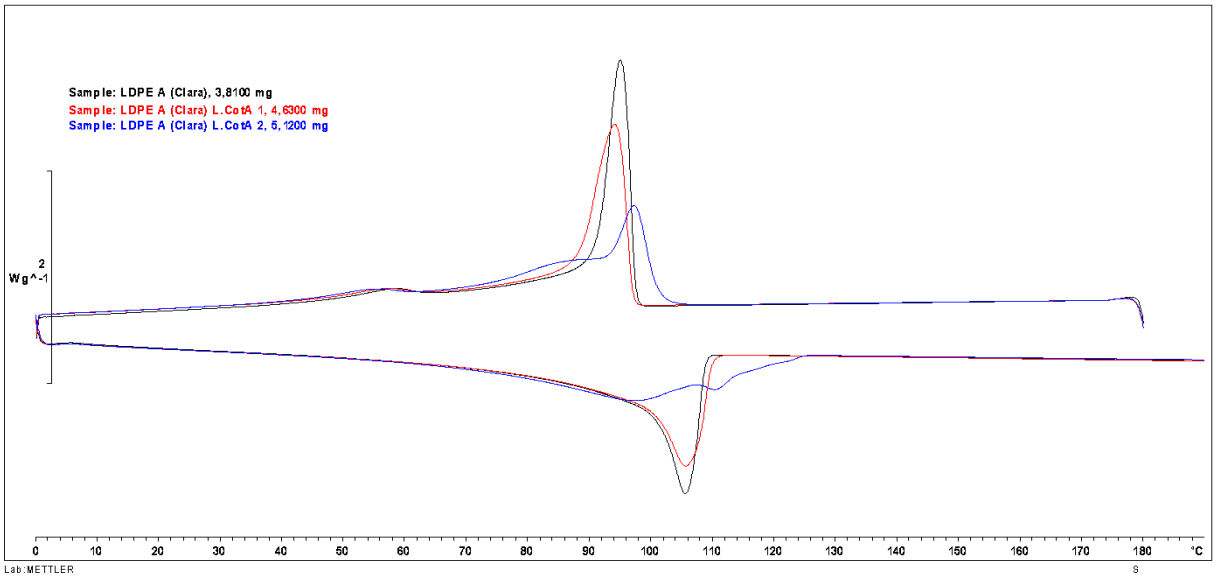

Figure A10: DSC curve from LDPEa samples with their respective mass. The black curve represents the untreated film, the red curve represents treatment with $KMnO_4$/HCl followed by L.CotA and the blue curve represents treatment with Fenton followed by L.CotA.

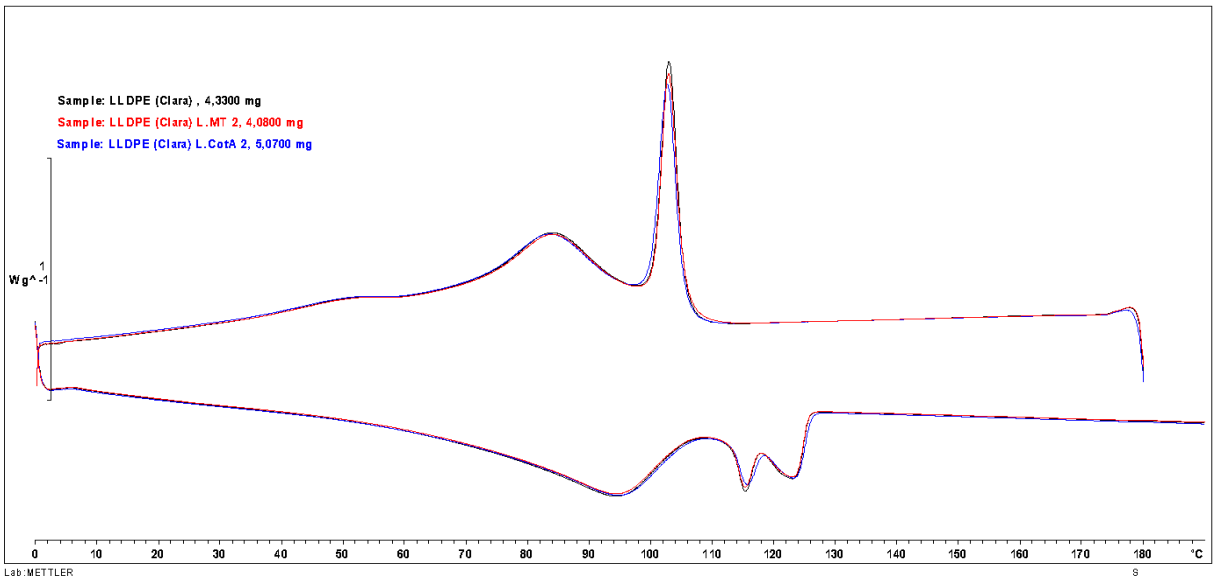

Figure A11: DSC curve from LLDPE samples with their respective mass. The black curve represents the untreated film, the red curve represents treatment with Fenton followed by L.MT and the blue curve represents treatment with Fenton followed by L.CotA.

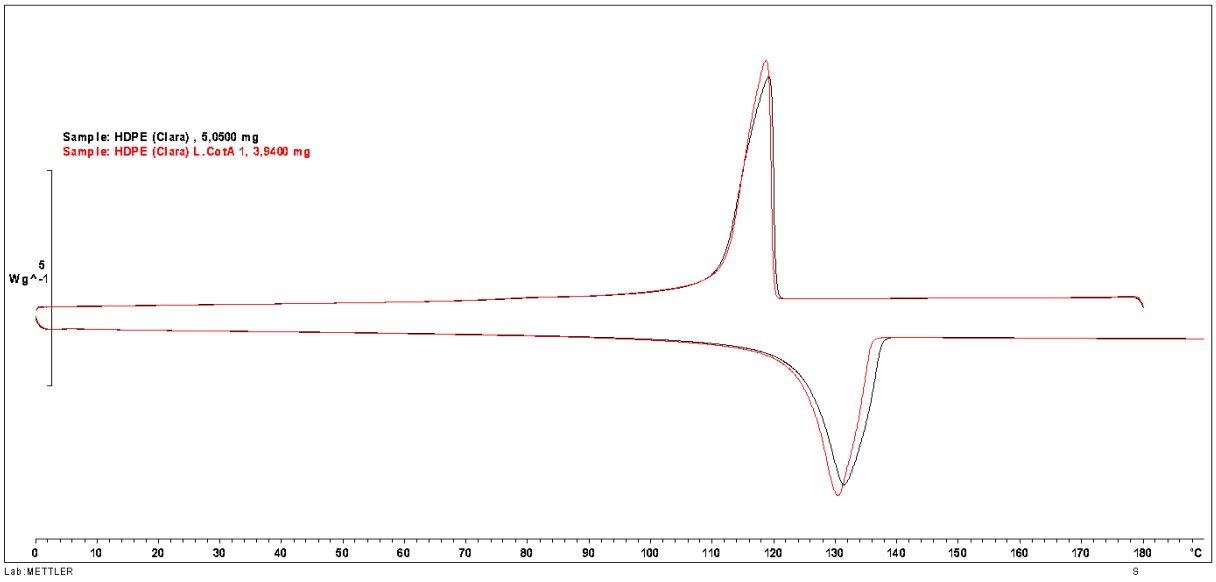

Figure A12: DSC curve from HDPE samples with their respective mass. The black curve represents the untreated film and the red curve represents treatment with O./HCl followed by L.CotA.

HPLC results

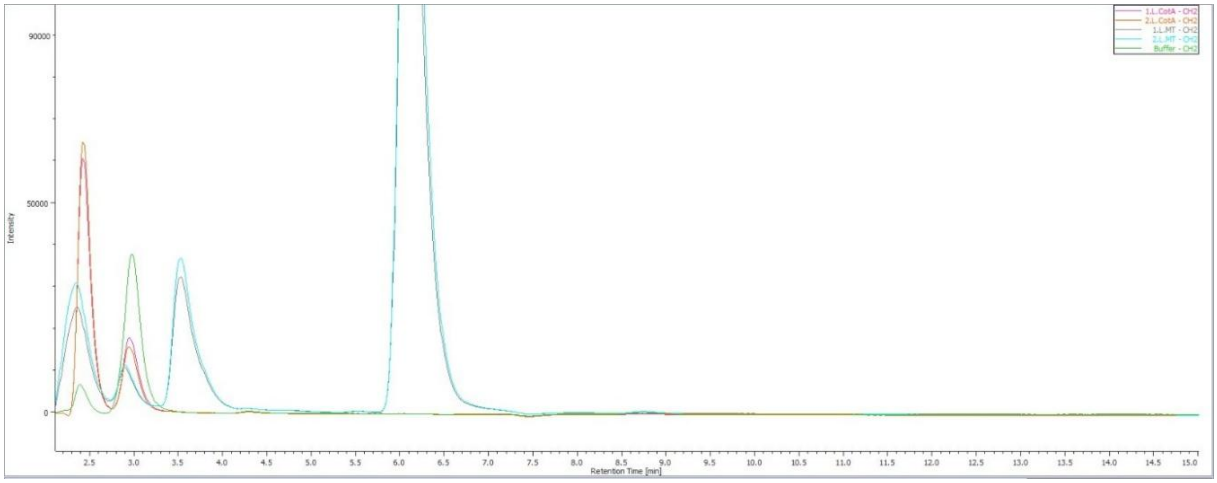

Figure A13: HPLC analysis of pooled reaction mixtures following chemoenzymatic treatment. Samples include treatment with $KMnO_4$/HCl followed by L.CotA (pink), Fenton oxidation followed by L.CotA (orange), $KMnO_4$/HCl followed by L.MT (brown), Fenton oxidation followed by L.MT (turquoise) and control sample (buffer with L.CotA, green).

GC-MS results

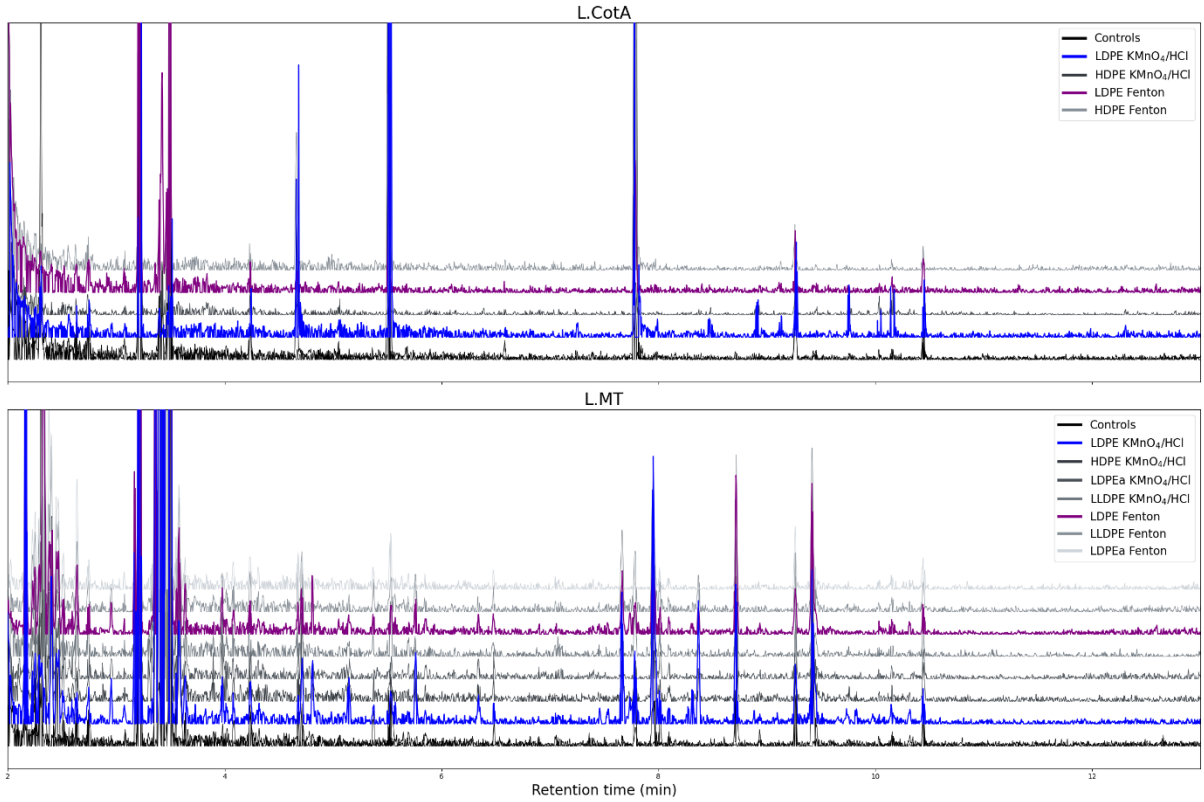

Figure A14: GC analysis of reaction mixture from additional films. The black curve represents the combined control samples(buffer with pretreated film without enzyme and buffer with enzyme without film). The blue curve represents LDPE treated with $KMnO_4$/HCl followed by L.CotA (top) and L.MT (bottom). The purple curve represents LDPE treated with Fenton oxidation followed by L.CotA (top) and L.MT (bottom). The grey curves represent the additional samples from LDPEa, LLDPE and HDPE.